TR - H - 167

Bifurcations in mean field theory annealing

Masa-aki Sato **Shin Ishii**

1995. 10. 4

ATR人間情報通信研究所

〒619-02 京都府相楽郡精華町光台2-2 ☎ 0774-95-1011

ATR Human Information Processing Research Laboratories
2-2, Hikaridai, Seika-cho, Soraku-gun, Kyoto 619-02 Japan
Telephone: +81-774-95-1011
Facsimile: +81-774-95-1008

Bifurcations in mean field theory annealing

Masa-aki Sato **Shin Ishii**

ATR Human Information Processing Research Laboratories

2-2 Hikaridai, Seika-cho, Soraku-gun, Kyoto 619-02, Japan

(TEL) +81-774-95-1039 (FAX) +81-774-95-1008

(E-mail) ishii@hip.atr.co.jp

Abstract

In this paper, we investigate bifurcation processes for the mean field theory (MFT) annealing applied to traveling salesman problems (TSPs). Due to the symmetries of the TSP free energy function, some special bifurcations occur: cyclic symmetry breaking bifurcations and reverse symmetry breaking bifurcations. Saddle-node bifurcations also occur. Which type of bifurcations occurs depends on the symmetry of the eigenvector that corresponds to the zero eigenvalue mode of the free energy curvature matrix at the bifurcation point. In the MFT annealing process, a sequence of bifurcations occurs and the bifurcation structure affects the quality of the annealing solution. It is shown that the annealing solution in this process is not unique in general, and it is not always the optimal solution. Our approach can also be applied to the Potts spin model and its bifurcation structure is almost the same as that of the MFT.

Acknowledgment

We thank Masaya Yamaguti of Ryukoku University for his valuable comments on symmetries and bifurcations, and for introducing literatures on bifurcations to us.

I Introduction

In his original paper, Hopfield [1] showed that a Lyapunov function can be defined for analog Hopfield network and the network always converges to a local minimum of the Lyapunov function. When the slope of the sigmoidal output function becomes very large, the Lyapunov function is nearly equal to the energy function, which has a quadratic form of the state variables. By utilizing this feature, the Hopfield network can be used for solving combinatorial optimization problems defined as minimizing of the quadratic energy function [2].

The physical meaning of the Hopfield network was further clarified by Peterson and Anderson [3, 4]. They showed that the Hopfield network is equivalent to the mean field theory (MFT) of the Boltzmann machine [5]. In this sense, the MFT can also be called a "Deterministic Boltzmann Machine" [6]. The Lyapunov function of the Hopfield network corresponds to the free energy function in the MFT. This implies that the Hopfield network converges to a local minimum of the free energy function in the MFT.

Wilson and Pawley [7] reported that the Hopfield network is not a good algorithm for solving combinatorial optimization problems when the problem scale becomes large. Therefore, neural network approaches need some additional mechanisms for relatively large-scale problems. One of them is MFT annealing [8, 9], i.e., the mean field version of simulated annealing [10]. The free energy function has a unique minimum at high temperature. By gradually lowering the temperature, one can get a relatively good local minimum at low temperature.

During the course of the annealing process, a sequence of bifurcations for minimum solutions occurs. The structure of the bifurcations affects the quality of the annealing solution. In this paper, we theoretically study bifurcation structures in the MFT annealing. Traveling salesman problems (TSPs) are mainly studied, as they are representative of combinatorial optimization problems. Note that symmetries in a problem affect the structure of the bifurcations [11]. Without structurally stable symmetries in a problem, one can generically expect only saddle-node bifurcations to occur. However, the free energy function for a TSP has two types of symmetries, i.e., cyclic and reverse symmetries. Due to these symmetries, special types of bifurcations occurs. They are called cyclic symmetry breaking bifurcations and reverse symmetry breaking bifurcations. In TSPs, the unique minimum at high temperature has such cyclic and reverse symmetries. In contrast, feasible minima at low temperature, which correspond to Hamilton paths, have no symmetries. Therefore, the symmetric minimum at high temperature bifurcates into equivalent minima with no symmetries or is annihilated at some temperature through the cyclic symmetry breaking bifurcations and the reverse symmetry breaking bifurcations as shown in Fig. 1. It should be added that new minima are mostly generated by saddle-node bifurcations as shown in Fig. 1.

If the annealing solution is annihilated at some temperature and there are more than two distinctive minima at this temperature, whatever minimum is obtained by the annealing is not unique due to the instability at the annihilation point. This implies that the annealing solution in the MFT annealing is not unique in general, although the procedure is deterministic. This reminds us of the situation in chaotic dynamics [12].

When new minima are generated, their free energy levels are higher than that of the global minimum at that temperature. However, the free energy levels of some minimum solutions may cross one another as the temperature is lowered. Therefore, the MFT annealing

procedure does not always give the optimal solution. As a consequence, the annealing solution in the MFT annealing is, in general, a not-so-bad solution and is not unique.

Peterson and Söderberg [9] proposed the Potts spin model for TSPs and showed that the performance of the Potts spin model with the annealing is comparable with the simulated annealing and some other conventional algorithms even for large-scale problems [13]. The bifurcation structure of the Potts spin model will be shown in this paper to be almost the same as that of the MFT.

This paper is organized as follows. In Sec. II, the mean field theory is briefly explained. In Sec. III, saddle-node bifurcations are studied. In Sec. IV, symmetries in TSPs are studied. In Sec. V, local bifurcations in a problem with cyclic and reverse symmetries are described. A typical example of the bifurcation diagram in the MFT annealing is shown; this example shows the non-optimality and non-uniqueness of the annealing solution. In Sec. VI, the Potts spin model is studied.

II Mean field theory

Many $\mathcal{NP}$-complete optimization problems can be described as a quadratic energy minimization problem for binary variables $S_n (= 0 \text{ or } 1)$:

$$E(\mathbf{S}) = \frac{1}{2} \sum_{n,m=1}^{N} W_{nm} S_n S_m + \sum_{n=1}^{N} J_n S_n. \tag{2.1}$$

In this formulation, constraints are treated as soft constraints, namely, the energy function (2.1) includes cost terms for constraint violations. The values of parameters W_{nm} and J_n are determined for each problem.

In order to obtain the global minimum of the energy function (2.1), simulated annealing [10] can be used. However, in many cases, simulated annealing for the energy function (2.1) is too time consuming. Another approach is to use the mean field theory (MFT).

The MFT [3, 6] is a mean field theory approximation for the Boltzmann machine [5], which is statistical mechanics with the energy function (2.1). In the MFT, analog variables $V_n \in [0, 1]$, which represent the probability that the binary variable S_n takes the value 1, are introduced. They are assumed to be independent variables. The MFT free energy $F(\mathbf{V})$ is given by

$$F(\mathbf{V}) = E(\mathbf{V}) + T \cdot H(\mathbf{V}), \tag{2.2a}$$

$$E(\mathbf{V}) = \frac{1}{2} \sum W_{nm} V_n V_m + \sum J_n V_n, \tag{2.2b}$$

$$H(\mathbf{V}) = \sum \left[V_n \log V_n + (1 - V_n) \log(1 - V_n) + \log 2 \right], \tag{2.2c}$$

where T and $(-H)$ correspond to the temperature and entropy, respectively. In the following, H is called entropy function. The term $\log 2$ in (2.2c) is added to let $H(\mathbf{V})$ satisfy $H(\mathbf{V}) \geq 0$. Then the free energy decreases as the temperature decreases. This MFT free energy function is identical to the Lyapunov function of the analog Hopfield model [1]. Statistical equilibrium corresponds to a minimum of the MFT free energy function F (2.2), where the following

stationary condition is satisfied:

$$\frac{\partial F}{\partial V_n} = \sum_{m=1}^{N} W_{nm} V_m + J_n + T \log\left(\frac{V_n}{1 - V_n}\right) = 0. \tag{2.3}$$

Introducing new variables U_n by $U_n = T \log(V_n/(1 - V_n))$, the stationary condition (2.3) can be rewritten as

$$U_n = -\sum_{m=1}^{N} W_{nm} V_m - J_n, \tag{2.4a}$$

$$V_n = G(U_n) \equiv \frac{1}{1 + e^{-U_n/T}}. \tag{2.4b}$$

The solution of this MFT equation [3] can be obtained by using the analog Hopfield model [1]:

$$\tau \frac{dU_n(t)}{dt} = -\frac{\partial F}{\partial V_n} = -U_n(t) - \sum W_{nm} V_m(t) - J_n, \tag{2.5a}$$

$$V_n(t) = G(U_n(t)), \tag{2.5b}$$

the asynchronous MFT equation [4]:

$$U_n(t+1) = -\sum W_{nm} V_m(t) - J_n, \tag{2.6a}$$

$$V_n(t+1) = G(U_n(t+1)), \tag{2.6b}$$

or the gradient field dynamics of the free energy:

$$\tau \frac{dV_n(t)}{dt} = -\frac{\partial F}{\partial V_n} = -T \log\left(\frac{V_n(t)}{1 - V_n(t)}\right) - \sum W_{nm} V_m(t) - J_n. \tag{2.7}$$

At the high temperature limit ($T \to \infty$), the free energy (2.2a) is dominated by the entropy term ($T \cdot H$) and there is a unique minimum as will be proved in a later section. At the low temperature limit ($T \to 0$), on the other hand, the free energy function F (2.2a) is nearly equal to the energy function E (2.2b). The minima of the energy function (2.2b) in the hyper cube region ($V_n \in [0, 1]$) coincide with those of the energy function (2.1) for binary variables, if we assume the condition

$$W_{nn} = 0 \qquad (n = 1, ..., N). \tag{2.8}$$

Therefore, at the low temperature limit, the local minima of the free energy function (2.2) correspond to those of the energy function (2.1). If the temperature is fixed at a low value, whatever local minima are found by using (2.5), (2.6), or (2.7) are completely dependent on the initial condition.

In order to get a good local minimum of the energy function E (2.1), the MFT annealing [8] can be used. First, the MFT equation (2.3) is solved at high temperature and a unique solution is obtained. Then after slightly lowering the temperature, the MFT equation (2.3) is solved again starting from the higher temperature solution. By continuing this process,

one can get a low temperature solution that corresponds to a local minimum of the energy function (2.1).

There are a couple of questions to this procedure. Is the annealing solution unique? Does the annealing solution correspond to the global minimum of the energy function (2.1)? In the following, we will study these questions.

III Bifurcations in the MFT annealing

III-A Free energy function

The entropy function H (2.2c) has special properties. The second derivative, i.e., the curvature of H is given by

$$\frac{\partial^2 H}{\partial V_n \partial V_m} = \frac{\delta_{nm}}{V_n(1-V_n)}, \tag{3.1}$$

where δ_{nm} is Kronecker's delta. Since

$$0 \leq V_n(1-V_n) \leq 1/4 \quad \text{for } 0 \leq V_n \leq 1, \tag{3.2}$$

the curvature matrix $(\partial^2 H/\partial V \partial V)$ can be written as

$$(\partial^2 H/\partial V \partial V) = 4 \cdot \mathbf{1} + (\text{ positive semi-definite matrix}), \tag{3.3}$$

where $\mathbf{1}$ is the identity matrix. The curvature matrix of the free energy function is given by

$$\frac{\partial^2 F}{\partial V_n \partial V_m} = W_{nm} + T\frac{\partial^2 H}{\partial V_n \partial V_m}. \tag{3.4}$$

Let ξ_{min} denote the minimum eigenvalue of the energy curvature matrix $\mathbf{W}$. ξ_{min} is negative if condition (2.8) is satisfied. When temperature T is greater than $(-\xi_{min}/4)$, the curvature of the free energy function, (3.4), is positive definite. This implies that the free energy function is convex and there is a unique minimum of the free energy. At the low temperature limit, the free energy has a lot of local minima. Therefore, at some critical temperature $T_c(\leq -\xi_{min}/4)$, a bifurcation of the minimum solution, which corresponds to the phase transition in statistical mechanics, occurs.

The gradient of H, i.e., $\partial H/\partial V_n = \log(V_n/(1-V_n))$, diverges at the boundary ($V_n = 0$ or 1). From the convexity of H and the finiteness of the energy gradient, it can be shown that the free energy decreases toward the interior direction with an infinite gradient at the boundary if $T > 0$. This implies that minima of the free energy function (2.2) are interior points and never occur at the boundary. Therefore, in any local analysis on minima of the free energy function, one can neglect the boundary constraint $0 \leq V_n \leq 1$.

The bifurcation of minimum solutions for the free energy function F (2.2) is equivalent to the bifurcation of the analog Hopfield model (2.5), whose Lyapunov function is given by the MFT free energy function (2.2), and a non-linear dynamical system with a gradient vector field $(-\partial F/\partial V)$ (2.7) [12]. However, stability of the stationary point in the asynchronous MFT equation (2.6) is, in general, different from that of the free energy function (2.2).

A minimum solution V_n^* at the critical temperature T_c satisfies the stationary condition (2.3). Near the bifurcation point (V_n^*, T_c), the free energy (2.2) can be expressed as a Taylor series with respect to $\delta V_n = V_n - V_n^*$, and $\epsilon = T - T_c$:

$$\begin{aligned} F(V,T) = F(V^* + \delta V, T_c + \epsilon) = \quad & F(V^*, T_c) + \tfrac{1}{2}\textstyle\sum_{n,m=1}^{N} M_{nm}\delta V_n \delta V_m \\ & + \tfrac{1}{3!}\textstyle\sum_{n=1}^{N} a[1]_n \delta V_n^3 + \tfrac{1}{4!}\sum_{n=1}^{N} a[2]_n \delta V_n^4 + \ldots \\ & + \epsilon \textstyle\sum_{n=1}^{N} b[1]_n \delta V_n + \tfrac{1}{2}\epsilon \sum_{n=1}^{N} b[2]_n \delta V_n^2 + \ldots, \end{aligned} \tag{3.5a}$$

where

$$M_{nm} = \frac{\partial^2 F}{\partial V_n \partial V_m} = W_{nm} + \frac{\delta_{nm} T_c}{V_n^*(1 - V_n^*)}, \tag{3.5b}$$

$$a[1]_n = \frac{\partial^3 F}{\partial V_n^3} = T_c \left(\frac{\partial^3 H}{\partial V_n^3}\right) = \frac{T_c(2V_n^* - 1)}{(V_n^*(1 - V_n^*))^2}, \tag{3.5c}$$

$$a[2]_n = \frac{\partial^4 F}{\partial V_n^4} = T_c \left(\frac{\partial^4 H}{\partial V_n^4}\right) = \frac{2T_c(3(V_n^*)^2 - 3V_n^* + 1)}{(V_n^*(1 - V_n^*))^3}, \tag{3.5d}$$

$$b[1]_n = \frac{\partial^2 F}{\partial V_n \partial T} = \frac{\partial H}{\partial V_n} = \log\left(\frac{V_n^*}{1 - V_n^*}\right), \tag{3.5e}$$

$$b[2]_n = \frac{\partial^3 F}{\partial V_n^2 \partial T} = \frac{\partial^2 H}{\partial V_n^2} = \frac{1}{V_n^*(1 - V_n^*)}. \tag{3.5f}$$

The stationary condition (2.3) becomes

$$\begin{aligned} 0 = \quad & \textstyle\sum_{m=1}^{N} M_{nm}\delta V_m + \tfrac{1}{2} a[1]_n \delta V_n^2 + \tfrac{1}{3!} a[2]_n \delta V_n^3 + \ldots \\ & + \epsilon b[1]_n + \epsilon b[2]_n \delta V_n + \ldots \ . \end{aligned} \tag{3.6}$$

III-B Saddle-node bifurcation

The bifurcation structure depends on a symmetry of the problem. In this section, we consider a case where there are no symmetries. A problem with symmetries will be considered in the later sections. If there are no symmetries, one can generically expect that the curvature matrix $\mathbf{M}$ of the free energy, (3.5b), will have a simple zero eigenvalue at the bifurcation point. Let $\mathbf{v} = [v_n]$ be the eigenvector for the zero eigenvalue. In this case, there are three types of bifurcations, namely, saddle-node type, transcritical type, and pitchfork type bifurcations [12].

According to the bifurcation theory [12], the necessary conditions for these bifurcations are as follows. If the conditions

$$\sum_{n=1}^{N} v_n \left(\frac{\partial^2 F}{\partial V_n \partial T}\right) = \sum v_n \left(\frac{\partial H}{\partial V_n}\right) = \sum_{n=1}^{N} v_n b[1]_n \neq 0, \tag{3.7a}$$

and

$$\sum_{n,m,k=1}^{N} v_n v_m v_k \left(\frac{\partial^3 F}{\partial V_n \partial V_m \partial V_k}\right) = T_c \sum v_n^3 \left(\frac{\partial^3 H}{\partial V_n^3}\right) = \sum_{n=1}^{N} v_n^3 a[1]_n \neq 0 \tag{3.7b}$$

are satisfied, saddle-node bifurcations occur. If the conditions

$$(3.7a) \implies = 0, \tag{3.8a}$$

$$\sum_{n,m}^{N} v_n v_m \left(\frac{\partial^3 F}{\partial V_n \partial V_m \partial T} \right) = \sum v_n^2 \left(\frac{\partial^2 H}{\partial V_n^2} \right) = \sum v_n^2 b[2]_n \neq 0, \tag{3.8b}$$

and (3.7b) are satisfied, transcritical bifurcations occur. If the conditions

$$(3.7b) \implies = 0, \tag{3.9a}$$

$$\sum_{n,m,n',m'}^{N} \left(\frac{\partial^4 F}{\partial V_n \partial V_m \partial V_{n'} \partial V_{m'}} \right) = T_c \sum v_n^4 \left(\frac{\partial^4 H}{\partial V_n^4} \right) = \sum v_n^4 a[2]_n \neq 0, \tag{3.9b}$$

and (3.8) are satisfied, pitchfork bifurcations occur. However, when no structural stable symmetries exist in the problem, conditions (3.8a) and (3.9a) are broken down by a slight change of the energy parameters, such that transcritical and pitchfork bifurcations become saddle-node bifurcations. Therefore, one can generically expect that only saddle-node bifurcations occur if there are no structurally stable symmetries in a problem.

In order to understand how the bifurcation of the minimum solution occurs, it is helpful to study the free energy function restricted in the center subspace [12] at the bifurcation point, which is a line defined by

$$V_n = x \cdot v_n + V_n^*, \quad x_1 \leq x \leq x_2$$

where x_1 and x_2 are determined by the requirement that this line segment should lie within the hyper cube ($V_n \in [0, 1]$). Then, the above-shown bifurcation conditions can be rewritten in terms of this reduced free energy function in the center subspace. The saddle-node conditions (3.7) can be rewritten as

$$\left. \frac{\partial^2 F}{\partial x \partial T} \right|_{x=0} = \left. \frac{dH}{dx} \right|_{x=0} \neq 0 \tag{3.10a}$$

$$\left. \frac{\partial^3 F}{\partial x^3} \right|_{x=0} = T_c \left. \frac{d^3 H}{dx^3} \right|_{x=0} \neq 0, \tag{3.10b}$$

which are equivalent to the saddle-node conditions for the reduced one-dimensional free energy. The conditions for the transcritical and pitchfork bifurcations are also equivalent to those of the reduced free energy. Therefore, which type of bifurcation occurs for the original free energy can be determined by studying the bifurcation behavior of the reduced free energy which is easily visualized. In the following, we will study how the reduced free energy landscape changes as T varies.

The first, the second, and the fourth derivative of entropy function H with respect to x are given by

$$\frac{dH}{dx} = \sum_{n=1}^{N} v_n \log \left(\frac{V_n}{1 - V_n} \right), \tag{3.11a}$$

$$\frac{d^2H}{dx^2} = \sum_{n=1}^{N} \left(\frac{v_n^2}{V_n(1-V_n)} \right) > 0, \tag{3.11b}$$

$$\frac{d^4H}{dx^4} = \sum_{n=1}^{N} \frac{v_n^4(3(V_n-1/2)^2+1/4)}{(V_n(1-V_n))^3} > 0. \tag{3.11c}$$

From (3.11b) and (3.11a), one can see that (dH/dx) is a monotonically increasing function and diverges at the boundary ($x = x_1$ or x_2). (3.11c) and (3.11b) show that (d^2H/dx^2) is a convex function and diverges at the boundary, indicating that (d^3H/dx^3) is negative in $x_1 < x < x_3$ and positive in $x_3 < x < x_2$ for some x_3. This implies that (dH/dx) has a negative curvature in $x_1 < x < x_3$ and has a positive curvature in $x_3 < x < x_2$. Therefore, the shape of (dH/dx) has a *tan*-like shape as shown in Fig. 2a.

The stationary condition (2.3) along this line is given by

$$\frac{dH}{dx} = -\frac{1}{T}\left(\frac{dE}{dx}\right) = \frac{\eta}{T}(x - x_0), \tag{3.12a}$$

$$x_0 = -\frac{\sum W_{nm} v_n V_m^* + \sum J_n v_n}{\sum W_{nm} v_n v_m}, \tag{3.12b}$$

$$\eta = -\sum_{n,m} W_{nm} v_n v_m. \tag{3.12c}$$

Since $\mathbf{v}$ is the eigenvector corresponding to the zero eigenvalue of $\mathbf{M}$ (3.5b) at the bifurcation point (V_n^*, T_c),

$$\eta = -\sum_{n,m=1}^{N} W_{nm} v_n v_m = T_c \sum_{n=1}^{N} \frac{v_n^2}{V_n^*(1-V_n^*)} > 0 \tag{3.13}$$

holds. Since the stationary condition is satisfied at the bifurcation point,

$$\left.\frac{dH}{dx}\right|_{x=0} = -\frac{\eta}{T_c} x_0 \tag{3.14}$$

also holds.

The stationary condition (3.12) can be solved graphically. Solutions of (3.12) are intersections of the two graphs, $y = dH/dx$ and $y = \eta(x - x_0)/T$. If the saddle-node condition (3.10) is satisfied, $x_0 \neq 0$ holds. The graphs, $y = dH/dx$ and $y = \eta(x - x_0)/T$ in this case are drawn in Fig. 2a. At the bifurcation point $x = 0$, the two graphs meet tangentially. From Fig. 2a, one can get the graph of $(\partial F/\partial x)$, Fig. 2b $\sim$ 2d. Then, the graphs of F (Fig. 2e) and $(\partial^2 F/\partial x^2)$ (Fig. 2f) follow. It can be seen that there is no stationary solution near the bifurcation point for $T > T_c$ and a stable and an unstable stationary point appear for $T < T_c$. This implies that a new minimum and an unstable saddle point are born at $T = T_c$ besides the existing minima as the temperature decreases as shown in Fig. 2g. At the birth of the new minimum, this minimum has a higher free energy than that of the global minimum at the critical temperature T_c. The graph of $(\partial^2 F/\partial x^2)$ in Fig. 2f shows that the condition $(\partial^3 F/\partial x^3)|_{x=0} \neq 0$, (3.10b), is satisfied.

There is another case whose figure is drawn in Fig. 3. In this case, a minimum disappears together with an unstable saddle point at $T = T_c$ as the temperature decreases.

If the saddle-node condition (3.10) is satisfied, the stationary condition (3.6) can be solved as a power series with respect to $\epsilon^{1/2}$. The leading order term can be calculated as

$$\delta V_n = x^* v_n \tag{3.15a}$$

$$(x^*)^2 = -\epsilon\kappa \tag{3.15b}$$

$$\kappa = \frac{2\sum v_n b[1]_n}{\sum v_n^3 a[1]_n} = \frac{2\left(dH/dx\right)|_{x=0}}{T_c\left(d^3H/dx^3\right)|_{x=0}}. \tag{3.15c}$$

This leading order of the stationary solution coincides with that of the reduced free energy. Therefore, stabilities of the stationary solutions are determined by those for the reduced one dimensional free energy drawn in Fig. 2 and Fig. 3. If $\kappa > 0$, there is no solution for $\epsilon > 0$ $(T > T_c)$ and there is a pair of solutions for $\epsilon < 0$ $(T < T_c)$. This corresponds to Fig. 2, where a new minimum is born as T decreases. If $\kappa < 0$, there is no solution for $\epsilon < 0$ $(T < T_c)$ and there is a pair of solutions for $\epsilon > 0$ $(T > T_c)$. This corresponds to Fig. 3, where a minimum disappears as T decreases.

IV TSP and symmetries

IV-A Cyclic and Reverse Symmetries in TSP

The bifurcation structure is affected by the symmetry of the problem [11]. In the following, we consider the traveling salesman problem (TSP) having a cyclic symmetry and a reverse symmetry. An energy function for the TSP is given by

$$\begin{aligned} E(\mathbf{V}) &= \frac{1}{2}\sum_{a,b,n,m=1}^{N_0} W_{a,n;b,m}V_{a,n}V_{b,m} + \sum_{a,n=1}^{N_0} J_{a,n}V_{a,n} + E_0 \\ &= \frac{1}{2}\sum_{a,b,n=1}^{N_0} D_{ab}V_{a,n}(V_{b,(n+1)} + V_{b,(n-1)}) \\ &\quad + \frac{A}{2}\left[\sum_a(\sum_n V_{a,n} - 1)^2 + \sum_n(\sum_a V_{a,n} - 1)^2 + 2\sum_{a,n} V_{a,n}(1 - V_{a,n})\right], \end{aligned} \tag{4.1}$$

where N_0 is the number of cities, $V_{a,n}$ represents the probability that the salesman visits city a at the n-th visit, and D_{ab} denotes the distance between city a and city b. This energy function is invariant under the cyclic permutation of the variable:

$$\mathbf{V} \longrightarrow \mathcal{T}_m^{[N_0]}\mathbf{V} \qquad (m = 1, ..., N_0 - 1), \tag{4.2a}$$

where $\mathcal{T}_m^{[N_0]}$ is the N_0-th order cyclic transformation operator defined by

$$(\mathcal{T}_m^{[N_0]}\mathbf{V})_{a,n} = V_{a,n+m} \qquad (a, n = 1, ..., N_0), \tag{4.2b}$$

$\mathcal{T}_{m+N_0}^{[N_0]} \equiv \mathcal{T}_m^{[N_0]}$ and $V_{a,n+N_0} \equiv V_{a,n}$. The energy function is also invariant under the reverse transformation:

$$\mathbf{V} \longrightarrow \mathcal{R}_m^{[N_0]}\mathbf{V} \qquad (m = 0, 1, ...N_0 - 1), \tag{4.3a}$$

where $\mathcal{R}_m^{[N_0]}$ is the N_0-th order reverse transformation operator defined by

$$(\mathcal{R}_m^{[N_0]}\mathbf{V})_{a,n} = V_{a,m-n} \qquad (a, n = 1, ..., N_0) \tag{4.3b}$$

and $\mathcal{R}_{m+N_0}^{[N_0]} \equiv \mathcal{R}_m^{[N_0]}$. The transformations (4.2) and (4.3) form a group:

$$\mathcal{T}_0^{[N_0]} = \mathbf{1} \text{ (identity operator)}, \tag{4.4a}$$
$$\mathcal{T}_m^{[N_0]}\mathcal{T}_n^{[N_0]} = \mathcal{T}_{m+n}^{[N_0]}, \tag{4.4b}$$
$$\mathcal{T}_m^{[N_0]}\mathcal{R}_n^{[N_0]} = \mathcal{R}_{m+n}^{[N_0]}, \tag{4.4c}$$
$$\mathcal{R}_m^{[N_0]}\mathcal{T}_n^{[N_0]} = \mathcal{R}_{m-n}^{[N_0]}, \tag{4.4d}$$
$$\mathcal{R}_m^{[N_0]}\mathcal{R}_n^{[N_0]} = \mathcal{T}_{m-n}^{[N_0]} \quad (n, m = 0, 1, ..., N_0 - 1). \tag{4.4e}$$

The entropy and the free energy functions are also invariant under these transformations. The cyclic permutation symmetry corresponds to the fact that the tour length does not depend on the starting city. The reverse symmetry corresponds to the fact that the tour length does not change when the tour direction is reversed.

There is a symmetric stationary solution V_a^* of the free energy function for any T:

$$V_{a,n}^* = V_a^* \qquad (a, n = 1, ..., N_0). \tag{4.5}$$

This can be proved as follows. The stationary condition for the symmetric solution can be derived from the reduced free energy function for the symmetric solution, which is given by

$$\begin{aligned} F_s/N_0 \;=\; & \sum_{a,b=1}^{N_0} D_{ab}V_aV_b + \frac{A}{2}[N_0\sum_a(V_a - 1/N_0)^2 + (\sum_a V_a - 1)^2 + 2\sum_a V_a(1 - V_a)] \\ & + T\sum_a[V_a \log V_a + (1 - V_a)\log(1 - V_a)]. \end{aligned} \tag{4.6}$$

Since this reduced free energy function has at least one minimum point for any T, the original free energy function also has a symmetric stationary solution for any T. Since the original free energy function has a unique minimum at the high temperature limit, the unique minimum must be this symmetric solution (4.5). Below the critical temperature, this symmetry breaks down to partially symmetric solutions or non-symmetric solutions.

If N_0 is decomposed as a product of two integers N_1 and N, i.e., $N_0 = N_1N$, a partially symmetric solution $\mathbf{V}$ having a symmetry:

$$V_{a,(n+kN_1)}^* = V_{a,n}^* \qquad (a = 1, ..., N_0; n = 1, ..., N_1; k = 1, ..., N - 1) \tag{4.7}$$

may appear. We call this symmetry the N-th order cyclic symmetry. This solution may or may not have the N-th order reverse symmetry:

$$V_{a,(m_0+kN_1-n)}^* = V_{a,n}^* \qquad (a, n = 1, ..., N_0; k = 0, 1, ..., N - 1) \tag{4.8}$$

for a specific m_0 ($1 \leq m_0 \leq N_1$) called a reflection point index. If there is a minimum solution with the N-th order cyclic and reverse symmetries, there must be N_1 equivalent minimum solutions due to the invariance of the free energy function under the N_0-th order cyclic and reverse transformations. They are related with each other by the N_1-th order cyclic transformation:

$$V_{a,n} \longrightarrow V_{a,n+m} \qquad (a, n = 1, ..., N_0; m = 1, ..., N_1 - 1). \tag{4.9}$$

Each solution has a different reflection point index m_0 ($1 \leq m_0 \leq N_1$) for the reverse symmetry (4.8). If they do not have the reverse symmetry, there must be $2N_1$ equivalent minimum solutions. They are related with each other by the N_1-th order cyclic transformation (4.9) and the N_1-th order reverse transformation:

$$V_{a,n} \longrightarrow V_{a,m-n} \qquad (a, n = 1, ..., N_0; m = 0, ..., N_1 - 1). \tag{4.10}$$

If one expands the free energy function around a minimum solution $\mathbf{V}^*$ with the N-th order cyclic symmetry, (4.7), with respect to $\delta V_{a,n} = V_{a,n} - V^*_{a,n}$, the free energy function $F(\mathbf{V}^* + \delta\mathbf{V})$ is invariant under the N-th order cyclic transformation:

$$\delta\mathbf{V} \longrightarrow \mathcal{T}_m^{[N]}\delta\mathbf{V} \qquad (m = 1, ..., N - 1), \tag{4.11a}$$

where the N-th order cyclic transformation operator $\mathcal{T}_m^{[N]}$ is defined by

$$(\mathcal{T}_m^{[N]}\mathbf{V})_{a,n} = (\mathcal{T}_{mN_1}^{[N_0]}\mathbf{V})_{a,n} = V_{a,(n+mN_1)} \quad (a, n = 1, ..., N_0) \tag{4.11b}$$

and $\mathcal{T}_{m+N}^{[N]} \equiv \mathcal{T}_m^{[N]}$. If the solution $\mathbf{V}^*$ has the N-th order reverse symmetry (4.8), the free energy function $F(\mathbf{V}^* + \delta\mathbf{V})$ is also invariant under the N-th order reverse transformation:

$$\delta\mathbf{V} \longrightarrow \mathcal{R}_m^{[N]}\delta\mathbf{V} \qquad (m = 0, 1, ..., N - 1), \tag{4.12a}$$

where the N-th order reverse transformation operator $\mathcal{R}_m^{[N]}$ is defined by

$$(\mathcal{R}_m^{[N]}\mathbf{V})_{a,n} = (\mathcal{R}_{m_0+mN_1}^{[N_0]}\mathbf{V})_{a,n} = V_{a,(m_0+mN_1-n)} \quad (a, n = 1, ..., N_0) \tag{4.12b}$$

and $\mathcal{R}_{m+N}^{[N]} \equiv \mathcal{R}_m^{[N]}$.

In order to make symmetric properties clear, it is convenient to change the numbering of the suffix (a, n). Let us define a vector variable $\tilde{\mathbf{V}}$ with the triple suffix (a, i, n) by

$$\tilde{V}_{a,i,n} \equiv V_{a,(i+(n-1)N_1)} \quad (a = 1, ..., N_0; i = 1, ..., N_1; n = 1, ..., N). \tag{4.13}$$

From the definition, $\tilde{V}_{a,i,n}$ satisfies the relations $\tilde{V}_{a,i,n+N} = \tilde{V}_{a,i,n}$ and $\tilde{V}_{a,i\pm N_1,n} = \tilde{V}_{a,i,n\pm 1}$. Then, the N-th order cyclic and reverse transformations can be expressed as

$$(\mathcal{T}_m^{[N]}\tilde{\mathbf{V}})_{a,i,n} = \tilde{V}_{a,i,n+m} \tag{4.14a}$$

$$(\mathcal{R}_m^{[N]}\tilde{\mathbf{V}})_{a,i,n} = \begin{cases} \tilde{V}_{a,m_0-i,m-n+2} & (m_0 > i \geq 1) \\ \tilde{V}_{a,m_0-i+N_1,m-n+1} & (N_1 \geq i \geq m_0) \end{cases} \tag{4.14b}$$

The suffix n corresponds to the N-th order cyclic symmetry, the suffix i corresponds to the broken cyclic symmetry and the suffix a is irrelevant to the symmetry property. In the following, we consider the bifurcation of a minimum solution with the N-th order cyclic symmetry (4.7). It may or may not have the N-th order reverse symmetry (4.8). Also, we use the renumbered variable $\tilde{V}_{a,i,n}$ and omit $\sim$.

IV-B Eigenmodes for the curvature matrix

As in the previous section, the curvature matrix $\mathbf{M}$ of the free energy function at the bifurcation point is given by

$$\begin{aligned} M_{a,i,n;b,j,m} &\equiv \left(\frac{\partial^2 F}{\partial V_{a,i,n}\partial V_{b,j,m}}\right)(\mathbf{V}^*, T_c) \\ &= W_{a,i,n;b,j,m} + \frac{\delta_{ab}\delta_{ij}\delta_{nm}T_c}{V^*_{a,i,n}(1-V^*_{a,i,n})} \\ &\quad (a,b=1,...,N_0; i,j=1,...,N_1; n,m=1,...,N). \end{aligned} \tag{4.15}$$

Because of the invariance under the N-th order cyclic transformation (4.14a), the curvature matrix has the symmetry:

$$\begin{aligned} M_{a,i,n;b,j,m} = M_{a,i,(n+k);b,j,(m+k)} = M_{a,i,N;b,j,(m-n)} \\ (a,b=1,...,N_0; i,j=1,...,N_1; n,m,k=1,...,N), \end{aligned} \tag{4.16a}$$

which can be expressed in a matrix form as:

$$\mathbf{M}\mathcal{T}_m^{[N]} = \mathcal{T}_m^{[N]}\mathbf{M}. \tag{4.16b}$$

Then, eigenvectors of the curvature matrix $\mathbf{M}$ are also eigenvectors of the N-th order cyclic transformation $\mathcal{T}_m^{[N]}$. The eigenmodes of this matrix are characterized by the N-th roots of 1:

$$\alpha(k) = \exp\left(\frac{2\pi k i}{N}\right), \quad \alpha(k)^N = 1, \quad \bar{\alpha}(k) = \alpha(k)^{-1} = \alpha(-k), \quad k \in \Gamma_N, \tag{4.17}$$

where $\Gamma_N = \{0, \pm 1, ..., \pm(N/2-1), N/2\}$ for even N, and $\Gamma_N = \{0, \pm 1, ..., \pm(N-1)/2\}$ for odd N. The eigenvector of $\mathbf{M}$ associated with $\alpha(k)$ can be written as

$$u_{a,i,n}(k) \equiv v_{a,i}(k)\cdot\alpha(k)^n \qquad (a=1,...,N_0; i=1,...,N_1; n=1,...,N), \tag{4.18}$$

which is also an eigenvector of the N-th order cyclic transformation:

$$\mathcal{T}_m^{[N]}\mathbf{u}(k) = \alpha(k)^m\mathbf{u}(k). \tag{4.19}$$

The reduced (N_0, N_1)-dimensional eigen equation for $v_{a,i}(k)$ is written as

$$\sum_{b=1}^{N_0}\sum_{j=1}^{N_1}\Omega_{a,i;b,j}(k)v_{b,j}(k) = \lambda(k)v_{a,i}(k) \qquad (a=1,...,N_0; i=1,...,N_1), \tag{4.20a}$$

$$\Omega_{a,i;b,j}(k) = \sum_{n=1}^{N} M_{a,i,N;b,j,n}\alpha(k)^n \qquad (a,b=1,...,N_0; i,j=1,...,N_1). \tag{4.20b}$$

Since $\mathbf{M}$ is a real symmetric matrix, $\mathbf{\Omega}(k)$ becomes a Hermite matrix: $\mathbf{\Omega}^\dagger(k) = \mathbf{\Omega}(k)$, where $\dagger$ denotes the Hermite conjugate, i.e., $\Omega^\dagger_{a,i;b,j} \equiv \bar{\Omega}_{b,j;a,i}$. Therefore, the eigenvalue $\lambda(k)$ is real. From (4.20b), $\mathbf{\Omega}(k)$ satisfies

$$\bar{\mathbf{\Omega}}(k) = \mathbf{\Omega}(-k), \tag{4.21}$$

which implies that $\bar{\mathbf{v}}(k) = \mathbf{v}(-k)$ and $\lambda(k) = \lambda(-k)$. Then, eigenvectors of $\mathbf{M}$, $(v_{a,i}(k)\alpha(k)^n)$ and $(\bar{v}_{a,i}(k)\alpha(-k)^n)$, have the same eigenvalue, so that an eigenvalue corresponding to complex $\alpha(k)$ is doubly degenerate and an eigenvalue corresponding to real $\alpha(k)(= 1 \text{ or} -1)$ is simple. Let $\{v_{a,i}(r,k)|r = 0, 1, ..., N_0N_1 - 1; k \in \Gamma_N\}$ and $\{\lambda(r,k)|r = 0, 1, ..., N_0N_1 - 1; k \in \Gamma_N\}$ be the complete set of the eigenvectors and the eigenvalues of (4.20), respectively. Let us define the eigenmode coordinate $z_{r,k}$ by

$$\delta V_{a,i,n} = \sum_{k\in\Gamma_N} \sum_{r=0}^{N_0N_1-1} z_{r,k} \cdot (v_{a,i}(r,k) \cdot \alpha(k)^n) \qquad (a = 1, ..., N_0N_1; n = 1, ..., N). \tag{4.22}$$

In terms of the eigenmode coordinate $z_{r,k}$, the N-th order cyclic transformation (4.14a) becomes

$$z_{r,k} \longrightarrow \mathcal{T}_m^{[N]} z_{r,k} = \alpha(k)^m z_{r,k} \qquad (m = 1, ..., N-1). \tag{4.23}$$

The eigenmode coordinate $z_{r,k}$ forms the irreducible representation of the cyclic symmetry group, whereas the original variable $\delta V_{a,i,n}$ forms the reducible representation. Since $\delta V_{a,i,n}$ is real and $\bar{v}_{a,i}(r,k) = v_{a,i}(r,-k)$, the relation:

$$\bar{z}_{r,k} = z_{r,-k} \tag{4.24}$$

holds.

If the minimum solution $\mathbf{V}^*$ has the N-th order reverse symmetry (4.8), $\mathbf{M}$ satisfies the relation

$$\mathcal{R}_m^{[N]}\mathbf{M} = \mathbf{M}\mathcal{R}_m^{[N]}. \tag{4.25}$$

Let us define a reverse transformation matrix $\hat{\mathcal{R}}(k)$ in the reduced space (a,i) by

$$\hat{\mathcal{R}}(k)_{a,i;b,j} \equiv (\alpha(k)^2\delta_{m_0-i,j} + \alpha(k)\delta_{m_0-i+N_1,j})\delta_{ab}. \tag{4.26}$$

Then, $\hat{\mathcal{R}}(k)$ satisfies

$$\hat{\mathcal{R}}^\dagger(k)\hat{\mathcal{R}}(k) = \mathbf{1} \ : \ \hat{\mathcal{R}}^{-1}(k) = \hat{\mathcal{R}}^\dagger(k). \tag{4.27}$$

From relation (4.25), it follows that

$$\hat{\mathcal{R}}(k)\mathbf{\Omega}(k) = \mathbf{\Omega}(-k)\hat{\mathcal{R}}(k). \tag{4.28}$$

This implies that

$$\hat{\mathcal{R}}(k)\mathbf{v}(r,k) = \chi(r,k)\mathbf{v}(r,-k), \tag{4.29}$$

where $\chi(r,k)$ is a complex number and satisfies $|\chi(r,k)|^2 = 1$ due to (4.27). $\chi(r,k)$ is called the reverse symmetry index. By using $\hat{\mathcal{R}}(k)$, the N-th order reverse transformation for the eigenvector of $\mathbf{M}$, $u_{a,i,n}(r,k) \equiv v_{a,i}(r,k)\alpha(k)^n$, can be written as

$$(\mathcal{R}_m^{[N]}\mathbf{u}(r,k))_{a,i,n} = \alpha(k)^m(\hat{\mathcal{R}}(k)\mathbf{v}(r,k))_{a,i}\alpha(-k)^n. \tag{4.30}$$

From (4.29), it can be proved that

$$\mathcal{R}_m^{[N]}\mathbf{u}(r,k) = \chi(r,k)\alpha(k)^m\mathbf{u}(r,-k). \tag{4.31}$$

Then, the N-th order reverse transformation (4.14b) for eigenmode coordinate $z_{r,k}$ becomes

$$z_{r,k} \longrightarrow \mathcal{R}_m^{[N]} z_{r,k} = \chi(r,k)\alpha(k)^m \bar{z}_{r,k}. \tag{4.32}$$

It should be noted that $\bar{z}_{r,k} = z_{r,k}$ and $\chi(r,k) = \pm 1$ for a real $\alpha(k)$ since $\mathbf{\Omega}(k) = \mathbf{\Omega}(-k)$, $\mathbf{v}(r,k) = \mathbf{v}(r,-k) = \bar{\mathbf{v}}(r,k)$ and $\hat{\mathcal{R}}(k)^2 = \mathbf{1}$ are satisfied for a real $\alpha(k)$.

V Bifurcations in TSP

V-A Saddle-node bifurcation

(a) $N = 1$ case

If the solution $\mathbf{V}^*$ at the bifurcation point has no symmetry, which corresponds to $N = 1$, the saddle-node bifurcation occurs as explained in Sec. III. In this case, $2N_0$ equivalent minima appear or disappear simultaneously by the saddle-node bifurcation due to the N_0-th order cyclic and reverse transformation invariance of the free energy function.

For a solution $\mathbf{V}^*$ with the N-th order cyclic symmetry, (4.7), the bifurcation structure depends on which eigenmode becomes a zero eigenvalue mode at the bifurcation point as described below.

(b) $\alpha(0)$ and no reverse symmetry case

First, let us assume that one of the eigenvectors with the N-th order cyclic symmetry, which corresponds to $\alpha(0)$ $(= 1)$, becomes a zero eigenvalue mode. Let $(r, k) = (0, 0)$ correspond to this zero eigenvalue mode. Since $\alpha(0)$ is real, this eigenvalue is simple. It is also assumed that the solution $\mathbf{V}^*$ has no reverse symmetry. The zero eigenvalue coordinate z_{00} does not change under the N-th order cyclic transformation (4.23). Then, the N-th order cyclic transformation invariance of the free energy does not give any special relation for the quantities, $\partial^2 F/\partial T \partial z_{00}$ and $\partial^3 F/\partial z_{00}^3$, which characterize the saddle-node condition (3.7). In this case, the saddle-node condition is generically satisfied:

$$\left.\frac{\partial^2 F}{\partial T \partial z_{00}}\right|_{z=0} = N \sum_{a=1}^{N_0} \sum_{i=1}^{N_1} b[1]_{a,i,1} v_{a,i}(0,0) \neq 0, \tag{5.1a}$$

$$\left.\frac{d^3 F}{dz_{00}^3}\right|_{z=0} = N \sum_{a=1}^{N_0} \sum_{i=1}^{N_1} a[1]_{a,i,1} v_{a,i}^3(0,0) \neq 0, \tag{5.1b}$$

where $b[1]_{a,i,1} = b[1]_{a,i,n} = \log(V^*_{a,i,1}/(1 - V^*_{a,i,1}))$ and $a[1]_{a,i,1} = a[1]_{a,i,n} = T_c(2V^*_{a,i,1} - 1)/(V^*_{a,i,1}(1 - V^*_{a,i,1}))^2$ as in (3.5). Therefore, $2N_1$ equivalent minima with the N-th order cyclic symmetry appear or disappear simultaneously by the saddle-node bifurcation.

(c) $\alpha(0)$, the reverse symmetry and $\chi = 1$ case

Let us consider the case that the minimum solution $\mathbf{V}^*$ at the bifurcation point also has the reverse symmetry. If the reverse symmetry index of the zero eigenvalue mode, $\chi(0, 0)$, is $+1$, the zero eigenvalue coordinate z_{00} does not change under the reverse transformation (4.32) since z_{00} is real. Then, the reverse transformation invariance of the free energy does not give any special relation for $\partial^2 F/\partial T \partial z_{00}$ and $\partial^3 F/\partial z_{00}^3$, and the saddle-node bifurcation occurs. In this case, N_1 equivalent minima with the N-th order cyclic and reverse symmetries appear or disappear simultaneously by the saddle-node bifurcation.

V-B Pitchfork bifurcation

(a) $\alpha(0)$, the reverse symmetry and $\chi = -1$ case

If the reverse symmetry index of the zero eigenvalue mode, $\chi(0,0)$, is -1, the zero eigenvalue coordinate z_{00} is transformed to $-z_{00}$ under the reverse transformation (4.32). Then, the reverse transformation invariance of the free energy gives the relation

$$\left.\frac{\partial^2 F}{\partial T \partial z_{00}}\right|_{z=0} = -\left.\frac{\partial^2 F}{\partial T \partial z_{00}}\right|_{z=0} = 0, \tag{5.2a}$$

$$\left.\frac{\partial^3 F}{\partial z_{00}^3}\right|_{z=0} = -\left.\frac{\partial^3 F}{\partial z_{00}^3}\right|_{z=0} = 0. \tag{5.2b}$$

This invariance does not give any relation for $\partial^3 F/\partial T \partial z_{00}^2$ and $\partial^4 F/\partial z_{00}^4$, and

$$\left.\frac{\partial^3 F}{\partial T \partial z_{00}^2}\right|_{z=0} = N \sum_{a=1}^{N_0} \sum_{i=1}^{N_1} b[2]_{a,i,1} v_{a,i}^2(0,0) \neq 0, \tag{5.3a}$$

$$\left.\frac{\partial^4 F}{\partial z_{00}^4}\right|_{z=0} = N \sum_{a=1}^{N_0} \sum_{i=1}^{N_1} a[2]_{a,i,1} v_{a,i}^4(0,0) \neq 0 \tag{5.3b}$$

are satisfied generically. The conditions (5.2) and (5.3) are nothing but the pitchfork conditions, (3.8) and (3.9). Therefore, the pitchfork bifurcation occurs. The relation (5.2) is structurally stable, since the reverse transformation invariance guarantees the relation even if the energy parameters are slightly changed.

The stationary condition (3.6) can be solved as a power series with respect to $\epsilon^{1/2}$. There is a solution with the N-th order cyclic and reverse symmetries for any T:

$$\delta V_{a,i,n}^s = -\epsilon \sum_{\chi(r,0)=1} \frac{1}{\lambda(r,0)} v_{a,i}(r,0) \left(\sum_{b=1}^{N_0} \sum_{j=1}^{N_1} b[1]_{b,j,1} v_{b,j}(r,0) \right) + O(\epsilon^2). \tag{5.4}$$

Let us define a constant Δ by

$$\Delta = \frac{\sum_{\chi(r,0)=1} (a[1]v^2(0,0)v(r,0))(b[1]v(r,0))/\lambda(r,0) - (b[2]v^2(0,0))}{\frac{1}{6}(a[2]v^4(0,0)) - \sum_{\chi(r,0)=1} (a[1]v^2(0,0)v(r,0))^2/(2\lambda(r,0))}, \tag{5.5}$$

where abbreviated notations $(a[1]v^2(0,0)v(r,0)) \equiv \sum_{a=1}^{N_0} \sum_{j=1}^{N_1} a[1]_{a,j,1} v_{a,j}^2(0,0) v_{a,j}(r,0)$, etc. are used. If $\Delta\epsilon > 0$, there is a pair of solutions:

$$\delta V_{a,i,n}^{\pm} = \pm\sqrt{\Delta\epsilon} v_{a,i}(0,0) + O(\epsilon). \tag{5.6}$$

This pair of solutions does not exist if $\Delta\epsilon < 0$. The pair of solutions has the N-th order cyclic symmetry but does not have the reverse symmetry. They are related with each other by the reverse transformation: $\mathcal{R}_m^{[N]} \delta \mathbf{V}^+ = \delta \mathbf{V}^-$. There are four types of bifurcation diagrams (Fig. 4). There is no symmetry breaking of the N-th order cyclic symmetry, i.e., all the solutions have the N-th order cyclic symmetry. On the other hand, the symmetry breaking of the reverse symmetry occurs in this case. In Fig. 4a, a minimum with the reverse symmetry

for $T > T_c$ becomes a saddle point for $T < T_c$ and a pair of minima without the reverse symmetry appears for $T < T_c$. In Fig. 4b, a pair of minima without the reverse symmetry for $T > T_c$ disappears at $T = T_c$, and a saddle point with the reverse symmetry for $T > T_c$ becomes a minimum with the reverse symmetry for $T < T_c$. In Fig. 4c, a saddle point with the reverse symmetry for $T > T_c$ becomes a minimum with the reverse symmetry for $T < T_c$. There is also a pair of saddle points without the reverse symmetry for $T < T_c$. In Fig. 4d, a minimum with the reverse symmetry for $T > T_c$ becomes a saddle point for $T < T_c$. There is also a pair of saddle points without the reverse symmetry for $T > T_c$.

(b) $\alpha(N/2)$ and no reverse symmetry case

If N is even, there is another real $\alpha(N/2)$ $(= -1)$. Let us assume that one of the modes corresponding to $\alpha(N/2)$ becomes a zero eigenvalue mode. This zero eigenvalue is simple. It is also assumed that the solution $\mathbf{V}^*$ has no reverse symmetry. Let $(r, k) = (0, N/2)$ correspond to this zero eigenvalue mode. The corresponding eigenvector is given by $(v_{a,i}(0, N/2)(-1)^n)$, which has the $(N/2)$-th order cyclic symmetry. The zero eigenvalue coordinate $z_{0,N/2}$ is transformed to $\pm z_{0,N/2}$ under the N-th order cyclic transformation. The N-th order cyclic transformation invariance of the free energy gives the relation,

$$\left.\frac{\partial^2 F}{\partial T \partial z_{0,N/2}}\right|_{z=0} = -\left.\frac{\partial^2 F}{\partial T \partial z_{0,N/2}}\right|_{z=0} = 0 \tag{5.7a}$$

$$\left.\frac{\partial^3 F}{\partial z_{0,N/2}^3}\right|_{z=0} = -\left.\frac{\partial^3 F}{\partial z_{0,N/2}^3}\right|_{z=0} = 0, \tag{5.7b}$$

as in (5.2). Therefore, the structurally stable pitchfork bifurcation occurs.

The stationary condition (3.6) can be solved as a power series with respect to $\epsilon^{1/2}$ as in (5.4). There is a solution with the N-th order cyclic symmetry for any T:

$$\delta V^s_{a,i,n} = -\epsilon \sum_{r=0}^{N_0 N_1 - 1} \frac{1}{\lambda(r,0)} v_{a,i}(r,0) \Big(\sum_{b=1}^{N_0}\sum_{j=1}^{N_1} b[1]_{b,j,1} v_{b,j}(r,0)\Big) + O(\epsilon^2). \tag{5.8}$$

Let us define a constant Δ by

$$\Delta = \frac{\sum_{r=0}^{N_0 N_1 - 1} (a[1]v^2(0,N/2)v(r,0))(b[1]v(r,0))/\lambda(r,0) - (b[2]v^2(0,N/2))}{\frac{1}{6}(a[2]v^4(0,N/2)) - \sum_{r=0}^{N_0 N_1 - 1}(a[1]v^2(0,N/2)v(r,0))^2/(2\lambda(r,0))}, \tag{5.9}$$

instead of (5.5). If $\Delta\epsilon > 0$, there is a pair of solutions:

$$\delta V^{\pm}_{a,i,n} = \pm\sqrt{\Delta\epsilon}\, v_{a,i}(0,N/2)(-1)^n + O(\epsilon). \tag{5.10}$$

This pair of solutions does not exist if $\Delta\epsilon < 0$. According to consideration on the N-th order cyclic transformation invariance, it can be proved that $z_{r,k} = 0$ for $k \neq 0, N/2$. Then, the pair of solutions $\delta V^{\pm}_{a,i,n}$ has the $(N/2)$-th order cyclic symmetry:

$$\delta V^{\pm}_{a,i,n+2m} = \delta V^{\pm}_{a,i,n} \qquad (a = 1, ..., N_0; i = 1, ..., N_1; n = 1, ..., N; m = 1, ..., N/2 - 1) \tag{5.11}$$

The solutions of the pair are related to each other by the 2nd order cyclic transformation: $\mathcal{T}_1^{[N]}\delta\mathbf{V}^+ = \delta\mathbf{V}^-$. There are four types of bifurcation diagrams (Fig. 4). In Fig. 4a, a minimum with the N-th order cyclic symmetry for $T > T_c$ becomes a saddle point for $T < T_c$ and a pair of minima with the $(N/2)$-th order cyclic symmetry appears for $T < T_c$. In Fig. 4b, a pair of minima with the $(N/2)$-th order cyclic symmetry for $T > T_c$ disappears at $T = T_c$, and a saddle point with the N-th order cyclic symmetry for $T > T_c$ becomes a minimum with the N-th order cyclic symmetry for $T < T_c$. In Fig. 4c, a saddle point with the N-th order cyclic symmetry for $T > T_c$ becomes a minimum with the N-th order cyclic symmetry for $T < T_c$. There is also a pair of saddle points with the $(N/2)$-th order cyclic symmetry for $T < T_c$. In Fig. 4d, a minimum with the N-th order cyclic symmetry for $T > T_c$ becomes a saddle point for $T < T_c$. There is also a pair of saddle points with the $(N/2)$-th order cyclic symmetry for $T > T_c$.

(c) $\alpha(N/2)$ and the reverse symmetry case

The presence of the reverse symmetry does not change the above bifurcation diagram. The symmetry breaking of the reverse symmetry does not occur even if the reverse symmetry index of the zero eigenvalue mode is -1. The pair of solutions $\delta\mathbf{V}^\pm$ has the reverse symmetry:

$$\mathcal{R}_{1+2m}^{[N]}\delta\mathbf{V}^\pm = \delta\mathbf{V}^\pm \quad \text{if} \quad \chi(0, N/2) = -1 \tag{5.12a}$$

$$\mathcal{R}_{2m}^{[N]}\delta\mathbf{V}^\pm = \delta\mathbf{V}^\pm \quad \text{if} \quad \chi(0, N/2) = 1 \tag{5.12b}$$

$$(m = 0, 1, ..., N/2 - 1),$$

which is the $(N/2)$-th order reverse symmetry.

V-C Symmetry breaking of cyclic symmetry

Next, we consider the case in which one of the modes corresponding to a complex $\alpha(K)$ ($K \in \Gamma_N, K \neq 0, N/2$) becomes a zero eigenvalue mode. This eigenvalue is doubly degenerate. In this subsection, we assume that there is no common divisor for K and N. In order to simplify the discussion, let us first consider a specific case, i.e., $N_1 = 1, N = 5, K = 1$ and the suffix a is neglected since it is not relevant to the symmetry properties. The index r is also omitted. In this case, the solution $\mathbf{V}^*$ has the reverse symmetry and the reverse symmetry indices of all the eigenmodes are $+1$. A more general case will be discussed later.

(a) $N = 5, \alpha(1)$, the reverse symmetry and $\chi = 1$ case

The free energy function $F(\mathbf{V}^* + \delta\mathbf{V}, T_c + \epsilon)$ in terms of the eigen coordinate $\{z_k | k = 0, \pm 1, \pm 2\}$ is given by

$$\begin{aligned} &F(\mathbf{V}^* + \delta\mathbf{V}, T_c + \epsilon)/5 = \\ &\quad \frac{1}{2}\lambda(0)z_0^2 + \lambda(2)\bar{z}_2 z_2 + \epsilon b[1]z_0 + \frac{1}{2}\epsilon b[2](z_0^2 + 2(\bar{z}_1 z_1 + \bar{z}_2 z_2)) \\ &\quad + \frac{1}{3!}a[1](z_0^3 + 6z_0(\bar{z}_1 z_1 + \bar{z}_2 z_2) + 3(z_1^2\bar{z}_2 + \bar{z}_1^2 z_2 + z_1 z_2^2 + \bar{z}_1\bar{z}_2^2)) \end{aligned} \tag{5.13}$$

$$+\frac{1}{4!}a[2]\{z_0^4+12z_0^2(\bar{z}_1z_1+\bar{z}_2z_2)+12z_0(\bar{z}_2z_1^2+z_2\bar{z}_1^2+z_1z_2^2+\bar{z}_1\bar{z}_2^2)$$
$$+6((\bar{z}_1z_1)^2+(\bar{z}_2z_2)^2+4(\bar{z}_1z_1)(\bar{z}_2z_2))+4(z_1^3z_2+\bar{z}_1^3\bar{z}_2+z_1\bar{z}_2^3+\bar{z}_1z_2^3)\}+\ldots\ .$$

Because of the invariance under the $N(=5)$-th order cyclic transformation (4.23) and the $N(=5)$-th order reverse transformation (4.32), only the invariant combinations under (4.23) and (4.32) appear in (5.13).

The solution of the stationary condition, $\partial F/\partial z_k=0$, can be calculated as a power series with respect to $\epsilon^{1/2}$. Note that in (5.13) the leading orders for z_0 are z_0^2 and ϵz_0, those for z_1 are $\epsilon(\bar{z}_1z_1)$, $z_0(\bar{z}_1z_1)$, and $(\bar{z}_1z_1)^2$, and those for z_2 are $(\bar{z}_2z_2)$ and $(\bar{z}_2z_1^2+z_2\bar{z}_1^2)$. This implies that the leading orders of the stationary solution are $z_0\sim\epsilon$, $(\bar{z}_1z_1)\sim\epsilon$, and $z_2\sim z_1^2$. Then the non-zero eigenvalue modes z_0 and z_2 are an order of ϵ. On the other hand, the zero eigenvalue mode z_1 is an order of $\epsilon^{1/2}$. The non-zero eigenvalue modes z_0 and z_2 can be expanded as

$$z_k=\sum_{s=2}^{\infty}z_k^{(s)}\qquad(k=0,2),\tag{5.14}$$

where $z_k^{(s)}$ is an order of $\epsilon^{s/2}$. By assuming that z_1 is an order of $\epsilon^{1/2}$, the stationary conditions for z_0 and z_2 can be solved successively, and z_k $(k=0,2)$ can be expressed in terms of z_1:

$$z_0=C_{0,1}^{(2)}\epsilon+C_{0,2}^{(2)}(\bar{z}_1z_1)+C_{0,1}^{(4)}\epsilon(\bar{z}_1z_1)+C_{0,2}^{(4)}(\bar{z}_1z_1)^2+C_{0,1}^{(5)}(z_1^5+\bar{z}_1^5)+\ldots\tag{5.15a}$$
$$z_2=C_{2,1}^{(2)}z_1^2+C_{2,1}^{(3)}\bar{z}_1^3+\epsilon C_{2,1}^{(4)}z_1^2+C_{2,2}^{(4)}z_1^2(\bar{z}_1z_1)+\ldots,\tag{5.15b}$$

where $C^{(s)}$'s are coefficients of order $\epsilon^{s/2}$ which can be determined by comparing the terms of order $\epsilon^{s/2}$ in $\partial F/\partial z_k=0$. Because of the invariance under the 5-th order cyclic transformation and the 5-th order reverse transformation, each term on the right hand side of (5.15) has the same transformation property as the left hand side. Substituting (5.15) into (5.13), one can get the effective free energy for the zero eigenvalue mode z_1:

$$F(z_1) = \frac{1}{2}d_1\epsilon(\bar{z}_1z_1)+\frac{1}{4}d_2(\bar{z}_1z_1)^2+\frac{1}{5}d_3(z_1^5+\bar{z}_1^5)+\ldots\tag{5.16a}$$
$$d_1/5 = 2b[2]-2a[1]b[1]/\lambda(0)\tag{5.16b}$$
$$d_2/5 = a[2]-2a^2[1]/\lambda(0)-a^2[1]/\lambda(2)\tag{5.16c}$$
$$d_3/5 = 5a^3[1]/(8\lambda^2(2))-5a[1]a[2]/(12\lambda(2))+a[3]/24.\tag{5.16d}$$

This corresponds to the effective free energy in the center manifold [12] defined by $\partial F/\partial z_k=0$ for $k=0,2$. The effective free energy function $F(z_1)$ is a function of the elementary invariant combinations, $(\bar{z}_1z_1)$ and $(z_1^5+\bar{z}_1^5)$ [11], because of the invariance under the 5-th order cyclic and reverse transformations. The leading order terms, $\epsilon(\bar{z}_1z_1)$ and $(\bar{z}_1z_1)^2$ in (5.16), are invariant under the continuous transformation:

$$z_1\longrightarrow e^{i\theta}z_1\qquad(0\le\theta<2\pi).\tag{5.17}$$

Therefore, the leading order solution is continuously degenerate. However, the higher order term, $(z_1^5+\bar{z}_1^5)$, which is not invariant under the continuous transformation (5.17) but invariant under (4.23), breaks this continuous degeneracy. Let us define a polar coordinate

(γ, ϕ) by

$$z_1 = \gamma e^{i\phi}, \qquad \gamma \geq 0, \ 0 \leq \phi < 2\pi. \tag{5.18}$$

Then, the free energy (5.16) can be written as

$$F(\gamma, \phi) = \frac{1}{2} d_1 \epsilon \gamma^2 + \frac{1}{4} d_2 \gamma^4 + \frac{2}{5} d_3 \gamma^5 \cos 5\phi + ... \tag{5.19}$$

The shape of the effective free energy (5.19) is shown in Fig. 5. The stationary conditions are given by

$$0 = \frac{\partial F}{\partial \gamma} = (d_1 \epsilon + d_2 \gamma^2 + 2 d_3 \gamma^3 \cos 5\phi + ...)\gamma \tag{5.20a}$$

$$0 = \frac{\partial F}{\partial \phi} = -2 d_3 \gamma^5 \sin 5\phi + ... \ . \tag{5.20b}$$

The equation (5.20) has a solution:

$$\gamma = 0 \tag{5.21}$$

for any ϵ, which has the 5-th order cyclic and reverse symmetries since it has only symmetric component z_0. If $(\epsilon d_1/d_2) < 0$, there is another set of solutions:

$$\gamma = \sqrt{(-d_1/d_2)\epsilon} + O(\epsilon) \tag{5.22a}$$

$$\phi = j\pi/5 \qquad (j = 0, 1, ..., 9) \ . \tag{5.22b}$$

The stability of these solutions is determined by the curvature matrix:

$$\partial^2 F/\partial \gamma^2 = d_1 \epsilon + 3 d_2 \gamma^2 + 8 d_3 \gamma^3 \cos 5\phi + ... \tag{5.23a}$$

$$\partial^2 F/\partial \phi^2 = -10 d_3 \gamma^5 \cos 5\phi + ... \tag{5.23b}$$

$$\partial^2 F/\partial \gamma \partial \phi = -10 d_3 \gamma^4 \sin 5\phi + ... \ . \tag{5.23c}$$

The curvature matrix of the symmetric solution, $\gamma = 0$, becomes

$$\partial^2 F/\partial \gamma^2 = d_1 \epsilon. \tag{5.24}$$

The symmetric solution is stable for $d_1 \epsilon > 0$, and unstable for $d_1 \epsilon < 0$. The curvature matrix for the set of solutions (5.22) becomes

$$\partial^2 F/\partial \gamma^2 = -2 d_1 \epsilon + O(\epsilon^{3/2}) \tag{5.25a}$$

$$\partial^2 F/\partial \phi^2 = -10 d_3 (-(d_1/d_2)\epsilon)^{5/2} \cos(j\pi) + O(\epsilon^3) \tag{5.25b}$$

$$\partial^2 F/\partial \gamma \partial \phi = 0. \tag{5.25c}$$

The stability with respect to ϕ depends on the sign of d_3. The curvature $(\partial^2 F/\partial \phi^2)$ becomes positive for j:even (odd) if $d_3 < 0$ (> 0). The stability with respect to γ is opposite to that of the symmetric solution. The curvature $(\partial^2 F/\partial \gamma^2)$ becomes positive for $d_1 \epsilon < 0$, and negative for $d_1 \epsilon > 0$. Let us denote j:even (odd) solutions by

$$z_1^e[J] = \gamma e^{i2\pi J/5} \tag{5.26a}$$

$$z_1^o[J] = \gamma e^{(i2\pi J/5) + (i\pi/5)} \qquad (J = 0, 1, ..., 4), \tag{5.26b}$$

where γ is given by (5.22a). Under the 5-th order cyclic and reverse transformations, they are transformed as

$$\mathcal{T}_m^{[5]} z_1^e[J] = \alpha(1)^m z_1^e[J] = z_1^e[J+m] \pmod 5 \tag{5.27a}$$
$$\mathcal{T}_m^{[5]} z_1^o[J] = \alpha(1)^m z_1^o[J] = z_1^o[J+m] \pmod 5 \tag{5.27b}$$
$$\mathcal{R}_m^{[5]} z_1^e[J] = \alpha(1)^m \bar{z}_1^e[J] = z_1^e[m-J] \pmod 5 \tag{5.27c}$$
$$\mathcal{R}_m^{[5]} z_1^o[J] = \alpha(1)^m \bar{z}_1^o[J] = z_1^o[m-J-1] \pmod 5. \tag{5.27d}$$

These solutions are related by the 5-th order cyclic transformations $\mathcal{T}_m^{[5]}$ and have no cyclic symmetry. From (5.27), it is proved that they have the 1st order reverse symmetry:

$$\mathcal{R}_{m[J]}^{[5]} z_1^e[J] = z_1^e[J] \quad \text{for } m[J] = 2J \pmod 5, \tag{5.28a}$$
$$\mathcal{R}_{m'[J]}^{[5]} z_1^o[J] = z_1^o[J] \quad \text{for } m'[J] = 2J+1 \pmod 5. \tag{5.28b}$$

Therefore, the cyclic symmetry is broken by this bifurcation while the reverse symmetry is preserved.

Four types of bifurcation diagrams are illustrated in Fig. 6. In Fig. 6a, a minimum with the 5-th order cyclic symmetry for $T > T_c$ becomes a saddle point with the 5-th order cyclic symmetry for $T < T_c$. Five minima appear together with five saddle points for $T < T_c$. These new minima are not symmetric with respect to the cyclic symmetry. In Fig. 6b, five minima without the cyclic symmetry for $T > T_c$ disappear together with five saddle points without the cyclic symmetry at $T = T_c$. A saddle point with the 5-th order cyclic symmetry for $T > T_c$ becomes a minimum with the 5-th order cyclic symmetry for $T < T_c$. In Fig. 6c, a saddle point with the 5-th order cyclic symmetry for $T > T_c$ becomes a minimum with the 5-th order cyclic symmetry for $T < T_c$. There are ten saddle points without the cyclic symmetry for $T < T_c$. In Fig. 6d, a minimum with the 5-th order cyclic symmetry for $T > T_c$ becomes a saddle point with the 5-th order cyclic symmetry for $T < T_c$. There are ten saddle points without the cyclic symmetry for $T > T_c$. All of the solutions have the reverse symmetry.

(b) $\alpha(K)$ and no reverse symmetry case

Almost the same argument can be made for a general case with arbitrary N_0 and N, where $N_0 = N_1 N$. First, let us assume there is no reverse symmetry, i.e., the minimum at the bifurcation point has no reverse symmetry. Let $(r,k) = (0,K)$ be the zero eigenvalue mode. The stationary solution can also be calculated as a power series with respect to $\epsilon^{1/2}$. Consideration on the order of ϵ indicates that the zero eigenvalue mode $z_{0,K}$ is an order of $\epsilon^{1/2}$, the symmetric modes $z_{r,0}$ are an order of ϵ, and all other modes are an order of ϵ or higher. (There is an exception, i.e., $N = 3$. In this case, the zero eigenvalue mode $z_{0,K}$ is an order of ϵ, since $(z_{0,K}^3 + \bar{z}_{0,K}^3)$ becomes a leading order term in the free energy.) The stationary conditions, $\partial F/\partial z_{r,k} = 0$ for $(r,k) \neq (0,K)$, can be solved in terms of ϵ and $z_{0,K}$ which is assumed to be an order of $\epsilon^{1/2}$. Due to the invariance under the N-th order cyclic transformation (4.23), $z_{r,k}$ can be expressed as

$$z_{r,0} = C_{r,0,1}^{(2)} \epsilon + C_{r,0,2}^{(2)} (\bar{z}_{0,K} z_{0,K}) + O(\epsilon^2) \tag{5.29a}$$

$$z_{r,K} = C^{(3)}_{r,K,1}\epsilon z_{0,K} + O(\epsilon^{5/2}) \qquad (r \neq 0) \tag{5.29b}$$

$$z_{r,k} = \begin{cases} C^{(l_1)}_{r,k,1} z^{l_1}_{0,K} + O(\epsilon^{1+l_1/2}) \\ \text{or} \\ C^{(l_2)}_{r,k,1} \bar{z}^{l_2}_{0,K} + O(\epsilon^{1+l_2/2}), \end{cases} \tag{5.29c}$$

where l_1 is the minimum integer that satisfies $l_1 K = k \,(\text{mod } N)$, and l_2 is the minimum integer that satisfies $-l_2 K = k \,(\text{mod } N)$. The leading order term is given by $z^{l_1}_{0,K}$ ($\bar{z}^{l_2}_{0,K}$) if $l_1 \leq l_2$ ($l_1 \geq l_2$). Substituting (5.29) into the free energy function, one can obtain the effective free energy for the zero eigenvalue mode $z_{0,K}$:

$$F(z_{0,K}) = \frac{1}{2} d_1 \epsilon (\bar{z}_{0,K} z_{0,K}) + \frac{1}{4} d_2 (\bar{z}_{0,K} z_{0,K})^2 + \ldots + \frac{1}{N}(d_3 z^N_{0,K} + \bar{d}_3 \bar{z}^N_{0,K}) + \ldots \,. \tag{5.30}$$

Because of the invariance under the N-th order cyclic transformation (4.23), the effective free energy function $F(z_{0,K})$ is a function of $(\bar{z}_{0,K} z_{0,K})$, $z^N_{0,K}$ and $\bar{z}^N_{0,K}$, if there is no reverse symmetry. The stationary solution of $\partial F / \partial z_{0,K} = 0$ can be obtained by using the same argument as in the $N = 5$ case. There is a symmetric solution for any ϵ:

$$z_{0,K} = 0. \tag{5.31}$$

If $(\epsilon d_1 / d_2) < 0$, there is another set of solutions:

$$z^e_{0,K}[J] = \gamma e^{(i2\pi J/N) - (i\phi_0/N)} \tag{5.32a}$$

$$z^o_{0,K}[J] = \gamma e^{(i2\pi J/N) + (i(\pi - \phi_0)/N)} \qquad (J = 0, 1, \ldots, N-1), \tag{5.32b}$$

where γ is given by (5.22a) and $d_3 = |d_3| e^{i\phi_0}$. The stabilities of these solutions are the same as in the $N = 5$ case. Under the N-th order cyclic transformation, they are transformed as

$$\mathcal{T}^{[N]}_m z^{e,o}_{0,K}[J] = \alpha(K)^m z^{e,o}_{0,K}[J] = z^{e,o}_{0,K}[J + mK] \quad (\text{mod } N). \tag{5.33}$$

They are transformed to each other by the N-th order cyclic transformations $\mathcal{T}^{[N]}_m$ and have no cyclic symmetry. Then, there are four types of bifurcation diagrams as shown in Fig. 6 like in the case of $N = 5$. The only difference is that $N = 5$ is replaced by an arbitrary N. For example, the bifurcation diagram in Fig. 6a corresponds to the situation in which a minimum with the N-th order cyclic symmetry for $T > T_c$ becomes a saddle point with the N-th order cyclic symmetry for $T < T_c$. N minima without the cyclic symmetry appear together with N saddle points without the cyclic symmetry for $T < T_c$. These solutions have no reverse symmetry.

(c) $\alpha(K)$, the reverse symmetry case

Now, we consider the effect of the reverse symmetry. Let us assume that the minimum solution at the bifurcation point has the reverse symmetry. In this case, the elementary invariant combinations under the reverse transformation (4.32) are $(\bar{z}_{0,K} z_{0,K})$ and $(z^N_{0,K} + \chi(0,K)^N \bar{z}^N_{0,K})$, since $|\chi(0,K)|^2 = 1$. The effective free energy function $F(z_{0,K})$ is the same

as in (5.30) except that $(d_3 z_{0,K}^N + d_3 \bar{z}_{0,K}^N)$ is replaced by $d_3(z_{0,K}^N + \chi(0,K)^N \bar{z}_{0,K}^N)$. There is a symmetric solution (5.31) for any ϵ. If $(\epsilon d_1/d_2) < 0$, there is another set of solutions

$$z_{0,K}^e[J] = \gamma e^{(i2\pi J/N)+(i\psi/2)} \tag{5.34a}$$

$$z_{0,K}^o[J] = \gamma e^{(i2\pi J/N)+(i\pi/N)+(i\psi/2)} \quad (J = 0, 1, ..., N-1), \tag{5.34b}$$

where γ is given by (5.22a) and $\chi(0,K) = e^{i\psi}$. The stabilities of these solutions are the same as in the $N = 5$ case. Their transformation properties under the N-th order cyclic transformation are the same as in (5.33). The solutions (5.34) are transformed to each other by the N-th order cyclic transformation $\mathcal{T}_m^{[N]}$ and have no cyclic symmetry. Under the N-th order reverse transformation, they are transformed as

$$\mathcal{R}_m^{[N]} z_{0,K}^e[J] = \chi(0,K)\alpha(K)^m \bar{z}_{0,K}^e[J] = z_{0,K}^e[mK - J] \pmod N \tag{5.35a}$$

$$\mathcal{R}_m^{[N]} z_{0,K}^o[J] = \chi(0,K)\alpha(K)^m \bar{z}_{0,K}^o[J] = z_{0,K}^o[mK - J - 1] \pmod N. \tag{5.35b}$$

From (5.35), it is proved that they have the 1st order reverse symmetry:

$$\mathcal{R}_{m[J]}^{[N]} z_{0,K}^e[J] = z_{0,K}^e[J] \text{ for } m[J]K = 2J \pmod N \tag{5.36a}$$

$$\mathcal{R}_{m'[J]}^{[N]} z_{0,K}^o[J] = z_{0,K}^o[J] \text{ for } m'[J]K = 2J + 1 \pmod N. \tag{5.36b}$$

Therefore, the reverse symmetry is not broken in this case. The bifurcation diagrams are the same as those without reverse symmetry except that all the solutions have the reverse symmetry.

V-D Partial symmetry breaking of cyclic symmetry

In Sec.V-C, it is assumed that there is no common divisor for K and N. In the following, it is assumed that the greatest common measure of N and K is Q (> 1). Let us define $R = N/Q$ and $P = K/Q$. Then, $NP = KR$ is satisfied and there is no common divisor for P and R. Main differences from the argument in Sec. V-C are the following.

1. Under the N-th order cyclic transformation (4.23), $z_{r,k}$ is transformed like $z_{r,k} \to \alpha(k)^m z_{r,k}$, while $z_{0,K}^l$ ($\bar{z}_{0,K}^l$) is transformed like $z_{0,K}^l \to \alpha(k)^{ml} z_{0,K}^l$ ($\bar{z}_{0,K}^l \to \alpha(k)^{-ml} \bar{z}_{0,K}^l$). The transformation factors are written as $\alpha(k)^m = e^{i2\pi(mk)/N}$ and $\alpha(K)^{ml} = e^{i2\pi(mlK)/N}$ ($\alpha(K)^{-ml} = e^{-i2\pi(mlK)/N}$). In order that $z_{0,K}^l$ ($\bar{z}_{0,K}^l$) is transformed like $z_{r,k}$, the condition $k = lK$ ($-lK$) (mod N) should be satisfied. If k is a multiple of Q, there is an l that satisfies this condition. If k is not a multiple of Q, this condition can not be satisfied for any l. Therefore, (5.29c) is replaced by

$$z_{r,k} = \begin{cases} C_{r,k,1}^{(l)} z_{0,K}^l & \text{if } k = lQ \\ 0 & \text{if } k \text{ is not a multiple of } Q. \end{cases} \tag{5.37}$$

Since $\alpha(k)^R = 1$ for $k = lQ$, the above solution satisfies the symmetry:

$$z_{r,k} = \alpha(k)^{mR} z_{r,k} \qquad (m = 1, ..., Q-1). \tag{5.38}$$

This corresponds to the Q-th order cyclic symmetry:

$$\mathcal{T}_m^{[Q]} z_{r,k} = z_{r,k} \qquad (m = 1, ..., Q-1), \tag{5.39}$$

where $\mathcal{T}_m^{[Q]} \equiv \mathcal{T}_{mR}^{[N]}$.

2. Since $\alpha(K)^R = 1$, elementary invariant combinations under the N-th order cyclic transformation (4.23) are given by $(\bar{z}_{0,K} z_{0,K})$, $z_{0,K}^R$ and $\bar{z}_{0,K}^R$. Then, the effective free energy function $F(z_{0,K})$ can be written as

$$F(z_{0,K}) = \frac{1}{2} d_1 \epsilon (\bar{z}_{0,K} z_{0,K}) + \frac{1}{4} d_2 (\bar{z}_{0,K} z_{0,K})^2 + ... + \frac{1}{R} (d_3 z_{0,K}^R + \bar{d}_3 \bar{z}_{0,K}^R) + ... \tag{5.40}$$

The set of solutions with the Q-th order cyclic symmetry (5.39) is given by

$$z_{0,K}^e[J] = \gamma e^{(i2\pi J/R) - (i\phi_0/R)} \tag{5.41a}$$

$$z_{0,K}^o[J] = \gamma e^{(i2\pi J/R) + (i(\pi - \phi_0)/R)} \qquad (J = 0, 1, ..., R-1), \tag{5.45b}$$

where γ is given by (5.22a) and $d_3 = |d_3| e^{i\phi_0}$. Under the N-th order cyclic transformation, the solutions are transformed as

$$\mathcal{T}_m^{[N]} z_{0,K}^{e,o}[J] = \alpha(K)^m z_{0,K}^{e,o}[J] = z_{0,K}^{e,o}[J + mP] \pmod{R}. \tag{5.46}$$

They are transformed to each other by $\mathcal{T}_m^{[N]}$ $(m = 1, ..., R-1)$, since P and R have no common divisor. The bifurcation diagrams are the same as in Sec.V-C, except that the N solutions in Sec.V-C are replaced by the R solutions with the Q-th order cyclic symmetry.

3. The effect of the reverse symmetry is the same as in Sec.V-C, if the role of N and K are replaced by R and P in (5.34) $\sim$ (5.36), respectively. The reverse symmetry is not broken. The bifurcation diagrams are the same as those without the reverse symmetry except that all the solutions have the reverse symmetry.

V-E Summary

The previous arguments can be summarized as follows. The MFT free energy for a TSP with N_0 cities is invariant under the N_0-th order cyclic transformation (4.2) and the reverse transformation (4.3). At high temperature ($T > -\xi_{min}/4$), there is a unique minimum of the free energy. This unique minimum has the N_0-th order cyclic symmetry and the reverse symmetry. In the MFT annealing process, one will follow this minimum solution to a sufficiently low temperature by gradual lowering of the temperature. As the temperature decreases, bifurcations of minimum solutions occur.

If N_0 is decomposed as $N_0 = N_1 N$, minima with the N-th order cyclic symmetry (4.7) may appear. These minima may or may not have the reverse symmetry (4.8). If they have the reverse symmetry, there must be N_1 equivalent minima with the N-th order cyclic and reverse symmetries, due to the N_0-th order cyclic and reverse transformation invariance. These minima are related to each other by the N_1-th order cyclic transformation. If they do

not have the reverse symmetry, there must be $2N_1$ equivalent minima with the N-th order cyclic symmetry due to the N_0-th order cyclic and reverse transformation invariance.

There are three types of bifurcations.

1. **Saddle-node bifurcation**
   $2N_1$ (N_1) equivalent minima with the N-th order cyclic symmetry (and the N-th order reverse symmetry) may appear or disappear simultaneously by the saddle-node bifurcation. In TSPs, most typically $2N_0$ (,i.e., $N_1 = N_0, N = 1$) non-symmetric equivalent minima appear.

2. **Reverse symmetry brealing bifurcation**
   The reverse symmetry may break by this bifurcation; it is one type of pitchfork bifurcation. The cyclic symmetry does not break by this bifurcation. There are four types of bifurcation diagrams as shown in Fig. 4. If there are N_1 equivalent minima with the N-th order cyclic and reverse symmetries, each minimum may bifurcate into a pair of minima without the reverse symmetry but with the N-th order cyclic symmetry (Fig. 4a). If there are $2N_1$ equivalent minima without the reverse symmetry but with the N-th order cyclic symmetry, N_1 pairs of minima may collide at the N_1 bifurcation points and new N_1 minima with the N-th order cyclic and reverse symmetries may appear (Fig. 4b). Also, N_1 equivalent minima with the N-th order cyclic and reverse symmetries may appear (Fig. 4c) or disappear (Fig. 4d) simultaneously.

3. **Cyclic symmetry breaking bifurcation**
   The cyclic symmetry may break by this bifurcation. The reverse symmetry does not break by this bifurcation. There are four types of bifurcation diagrams as shown in Fig. 6. Let us assume N is further decomposed as $N = R \cdot Q$. If there are $2N_1$ (N_1) equivalent minima with the N-th order cyclic symmetry (and the N-th order reverse symmetry), each minimum may bifurcate into R equivalent minima with the Q-th order cyclic symmetry (and the Q-th order reverse symmetry) (Fig. 6a). If there are $2N_1$ (N_1) equivalent sets of R minima with the Q-th order cyclic symmetry (and the Q-th order reverse symmetry), $2N_1$ (N_1) sets of R minima collide at the $2N_1$ (N_1) bifurcation points and new $2N_1$ (N_1) minima with the N-th order cyclic symmetry (and the N-th order reverse symmetry) may appear (Fig. 6b). Also, $2N_1$ (N_1) equivalent minima with the N-th order cyclic symmetry (and the N-th order reverse symmetry) may appear (Fig. 6c) or disappear (Fig. 6d) simultaneously.

If the annealing solution bifurcates into N_1 (or $2N_1$) minima with the N-th order cyclic symmetry, one can follow the annealing solution since these minima are equivalent to each other. If the annealing solution is annihilated and there are more than two distinctive local minima having lower free energy values than the annihilation point at that temperature, one may not uniquely follow the annealing solution because of the instability at the annihilation point. Whether the annealing solution is unique or not depends on the basin structure of the local minima. Therefore, the MFT annealing procedure does not necessarily give a unique minimum solution in general, even though the procedure is deterministic.

When new minima appear, these local minima have a higher free energy than that of the global minima at that temperature. However, free energy levels of local minima may

cross each other as the temperature decreases. Therefore, the MFT annealing procedure does not guarantee the optimal solution. As a consequence, the annealing solution in the MFT annealing is, in general, a not-so-bad solution and is not unique.

V-F Example

Let us show a typical example of a bifurcation diagram. Figure 7a is a bifurcation diagram of a 5-city TSP, where $V_{1,i}$ $(i = 1, ..., 5)$ for every minimum are plotted against temperature. Figure 7b is the corresponding free energy diagram. In the experiment, the parameter A in (4.1) is set to be 1.5.

At high temperature, i.e., $T > 0.52$, there is a unique minimum (a). This minimum has the 5th order cyclic and reverse symmetries. At $T_1 \approx 0.52$, a saddle-node bifurcation occurs. Since all new minima have neither the cyclic symmetry nor the reverse symmetry, 10 non-symmetric minima (b) appear simultaneously. Since the new born minima (b) are local minima, their free energy level must be higher than that of the symmetric minimum (a) at the bifurcation temperature. However, the former becomes lower than the latter as the temperature is lowered. This free energy crossing occurs at $T \approx 0.518$ as seen in Fig. 7b. At $T_2 \approx 0.50$, another saddle-node bifurcation occurs, and 10 non-symmetric minima (c) appear. At $T_3 \approx 0.48$, a cyclic symmetry breaking bifurcation occurs. The minimum (a) with the 5th order cyclic and reverse symmetries bifurcates into five minima (d) without the cyclic symmetry but with the 1st order reverse symmetry. Because of the reverse symmetry, there are only three cascades observed in Fig. 7a. At $T_4 \approx 0.475$, a reverse symmetry breaking bifurcation occurs, and each of the five minima with the 1st order reverse symmetry (d) collides with saddle-points and eventually becomes a saddle-point. After this bifurcation, the original annealing solutions disappear. At this temperature, there exist two sets of minima, (b) and (c), and the free energy levels of these minima are lower than that of the disappearing minima as shown in Fig. 7b. In this case, due to the instability of the disappearing bifurcation point, which minimum is found is ambiguous, even if the procedure is deterministic. This example shows the non-uniqueness of the MFT annealing solution.

VI MFT annealing of Potts spin model

VI-A MFT for Potts spin model

A Potts spin model [9, 14] for a TSP is defined by an energy function:

$$\begin{aligned} E(\mathbf{S}) &= \frac{1}{2}\sum_{a,b,n,m=1}^{N_0} W_{a,n;b,m}S_{a,n}S_{b,m} + \sum_{a,n=1}^{N_0} J_{a,n}S_{a,n} \qquad (6.1)\\ &= \frac{1}{2}\sum_{a,b,n=1}^{N_0} D_{ab}S_{a,n}(S_{b,n+1}+S_{b,n-1}) + \frac{A}{2}\sum_{n=1}^{N_0}(\sum_{a=1}^{N_0} S_{a,n}-1)^2 + \frac{B}{2}\sum_{a=1}^{N_0}\sum_{n\neq m}^{N_0} S_{a,n}S_{a,m}, \end{aligned}$$

where Potts spin variables $S_{a,n}$ $(= 1$ or $0)$ satisfy the constraints:

$$\sum_{n=1}^{N_0} S_{a,n} = 1 \qquad (a = 1, ..., N_0). \qquad (6.2)$$

The MFT free energy for the Potts spin model (6.1) is given by

$$F(\mathbf{V}) = E(\mathbf{V}) + TH(\mathbf{V}), \tag{6.3a}$$

$$E(\mathbf{V}) = \frac{1}{2}\sum_{a,b,n,m=1}^{N_0} W_{a,n;b,m}V_{a,n}V_{b,m} + \sum_{a,n=1}^{N_0} J_{a,n}V_{a,n}, \tag{6.3b}$$

$$H(\mathbf{V}) = \sum_{a,n=1}^{N_0} V_{a,n}\log V_{a,n}, \tag{6.3c}$$

where the analog variables $V_{a,n} \in [0,1]$ represent the probability that $S_{a,n}$ takes a value 1 and satisfies the constraint:

$$\sum_{n=1}^{N_0} V_{a,n} = 1 \qquad (a = 1, ..., N_0). \tag{6.4}$$

Both the free energy function (6.3) and the constraint (6.4) are invariant under the N_0-th order cyclic transformation (4.2) and the N_0-th order reverse transformation (4.3). Therefore, minima with the N-th order cyclic symmetry (4.7) may appear if $N_0 = NN_1$. They may or may not have the N-th order reverse symmetry (4.8). If they have the reverse symmetry, there must be N_1 equivalent minima due to the N_0-th order cyclic transformation invariance as in Sec. V . If they do not have the reverse symmetry, there must be $2N_1$ equivalent minima due to the N_0-th order cyclic and reverse transformation invariance.

The gradient and the curvature of the entropy function (6.3c) are given by

$$\frac{\partial H}{\partial V_{a,n}} = \log V_{a,n} + 1, \tag{6.5a}$$

$$\frac{\partial^2 H}{\partial V_{a,n}\partial V_{b,m}} = \delta_{ab}\delta_{nm}\frac{1}{V_{a,n}}. \tag{6.5b}$$

Since some values of $V_{a,n}$ are zero at the boundary, the gradient of H, (6.5a), diverges at the boundary. Since $1/V_{a,n} \geq 1$, $H(\mathbf{V})$ is a convex function. Then, the same argument as in Sec. III-A can be made. Namely, a minimum of the free energy function (6.3) with the constraint (6.4) occurs at the interior point and one can neglect the boundary constraint $0 \leq V_{a,n} \leq 1$ in the local analysis of the minima.

Let us define a new coordinate $y_{a,k}$ by

$$V_{a,n} = \frac{1}{N_0}\sum_{k\in\Gamma_{N_0}} y_{a,k}\alpha(k)^n \qquad (a, n = 1, ..., N_0), \tag{6.6}$$

where $\alpha(k)$ is defined by (4.17) with $N = N_0$. Since $V_{a,n}$ is real and $\bar{\alpha}(k) = \alpha(-k)$,

$$\bar{y}_{a,k} = y_{a,-k} \qquad (a = 1, ..., N_0; k \in \Gamma_{N_0}) \tag{6.7}$$

is satisfied. By using the relation:

$$\sum_{n=1}^{N_0} \alpha(k)^n = 0 \qquad \text{for } k \neq 0, k \in \Gamma_{N_0}, \tag{6.8}$$

the constraint (6.4) can be explicitly solved as:

$$\sum_{n=1}^{N_0} V_{a,n} = y_{a,0} = 1 \quad (a = 1, ..., N_0). \tag{6.9}$$

Then, the problem is reduced to finding the minimum of the free energy function (6.3), in which $y_{a,0}$ is fixed to be 1, with respect to $y_{a,k}$ for $k \neq 0$. The free energy is still invariant under the N_0-th order cyclic transformation:

$$y_{a,k} \longrightarrow \mathcal{T}_m^{[N_0]} y_{a,k} = \alpha(k)^m y_{a,k} \quad (a, m = 1, ..., N_0; k \neq 0, k \in \Gamma_{N_0}) \tag{6.10}$$

and the N_0-th order reverse transformation:

$$y_{a,k} \longrightarrow \mathcal{R}_m^{[N_0]} y_{a,k} = \alpha(k)^m \bar{y}_{a,k} \quad (a = 1, ..., N_0; m = 0, ..., N_0 - 1; k \neq 0, k \in \Gamma_{N_0}). \tag{6.11}$$

Near the bifurcation point $(\mathbf{V}^*, T_c)$, which has the N-th order cyclic symmetry (4.7), one can define eigenmode coordinate $z_{r,k}$ as in Sec. IV-B by using the eigenvectors of the curvature matrix $(\partial^2 F/\partial V \partial V)(\mathbf{V}^*, T_c)$. The transformation properties of the eigenmode coordinate $z_{r,k}$ under the N-th order cyclic and reverse transformations are the same as in (4.23) and (4.32). The analysis for the bifurcation of the minimum solution can be done in the same way as in Sec. V. The only difference is that the N_0-th order cyclic symmetry mode $y_{a,0}$ is fixed by the constraint (6.9). Therefore, the minimum solution with the N_0-th order cyclic symmetry can not appear or disappear by the saddle-node bifurcation. Other types of bifurcations as described in Sec. V can also occur in this model.

VII Conclusion

In this paper, we investigated the MFT bifurcation processes for MFT applied to traveling salesman problems. Due to the cyclic and reverse symmetries of the TSP free energy function, some special bifurcations occur: cyclic symmetry breaking bifurcations and reverse symmetry breaking bifurcations. Saddle-node bifurcations also occur. Which type of bifurcations occurs depends on the symmetry of the eigenvector that corresponds to the zero eigenvalue mode of the free energy curvature matrix at the bifurcation point. In the MFT annealing process, a sequence of the above-mentioned bifurcations occurs and the bifurcation structure affects the quality of the annealing solution. The annealing solution in the MFT annealing is not unique in general, although the procedure is deterministic. Moreover, the MFT annealing procedure does not always give the optimal solution. As a consequence, the annealing solution is, in general, a not-so-bad solution and is not unique. Our approach can also be applied to the Potts spin model and its bifurcation structure is almost the same as that of the MFT.

References

[1] Hopfield, J. J. (1984). Neurons with graded responses have collective computational properties like those of two-state neurons. *Proceedings of the National Academy of Science USA*, **81**, 3088-3092.

[2] Hopfield, J. J., and Tank, D. W. (1985). "Neural" computations of decisions in optimization problems. *Biological Cybernetics*, **52**, 141-152.

[3] Peterson, C., and Anderson, J. R. (1987). A mean field theory learning algorithm for neural networks. *Complex Systems*, **1**, 995-1019.

[4] Peterson, C., and Anderson, J. R. (1988). Neural networks and NP-complete optimization problems: A performance study on the graph bisection problem. *Complex Systems*, **2**, 59-89.

[5] Ackley, D. H., Hinton, G. E., and Sejnowski, T. J. (1985). A learning algorithm for Boltzmann machines. *Cognitive Science*, **9**, 147-169.

[6] Hinton, G. E. (1989) Deterministic Boltzmann learning performs steepest descent in weight-space. *Neural Computation* **1**, 143-150.

[7] Wilson, G. W., and Pawley, G. S. (1988). On the stability of the travelling salesman problem algorithm of Hopfield and Tank. *Biological Cybernetics*, **58**, 63-70.

[8] Bilbro, G., Mann, R., Miller, T. K., Sydner, W. E., Van den Bout, D. E., and White, M. (1989). Optimization by mean field annealing. In *Advances in Neural Information Processing Systems I* (Denver 1988), ed. D. S. Touretzky, 91-98. San Mateo: Morgan Kaufmann.

[9] Peterson, C., and Söderberg, B. (1989). A new method for mapping optimization problems onto neural networks. *International Journal of Neural Systems*, **1**, 3-22.

[10] Kirkpatrick, S., Gelatt, C. D., and Vecchi, M. P. (1983). Optimization by simulated annealing. *Science*, **220**, 671-680.

[11] Golubitsky, M., Stewart, I., and Schaeffer, D. G. (1988). *Singularities and groups in bifurcation theory, Volume II*, Springer-Verlag (New York).

[12] Guckenheimer, J., and Holmes, P. (1983). *Nonlinear oscillations, dynamical systems, and bifurcations of vector fields*, Springer-Verlag (New York).

[13] Peterson, C. (1990). Parallel distributed approaches to combinatorial optimization: benchmark studies on traveling salesman problem. *Neural Computation*, **2**, 261-269.

[14] Van den Bout, D. E., and Miller III, T. K. (1989). Improving the performance of the Hopfield-Tank neural network through normalization and annealing. *Biological Cybernetics*, **62**, 129-139.

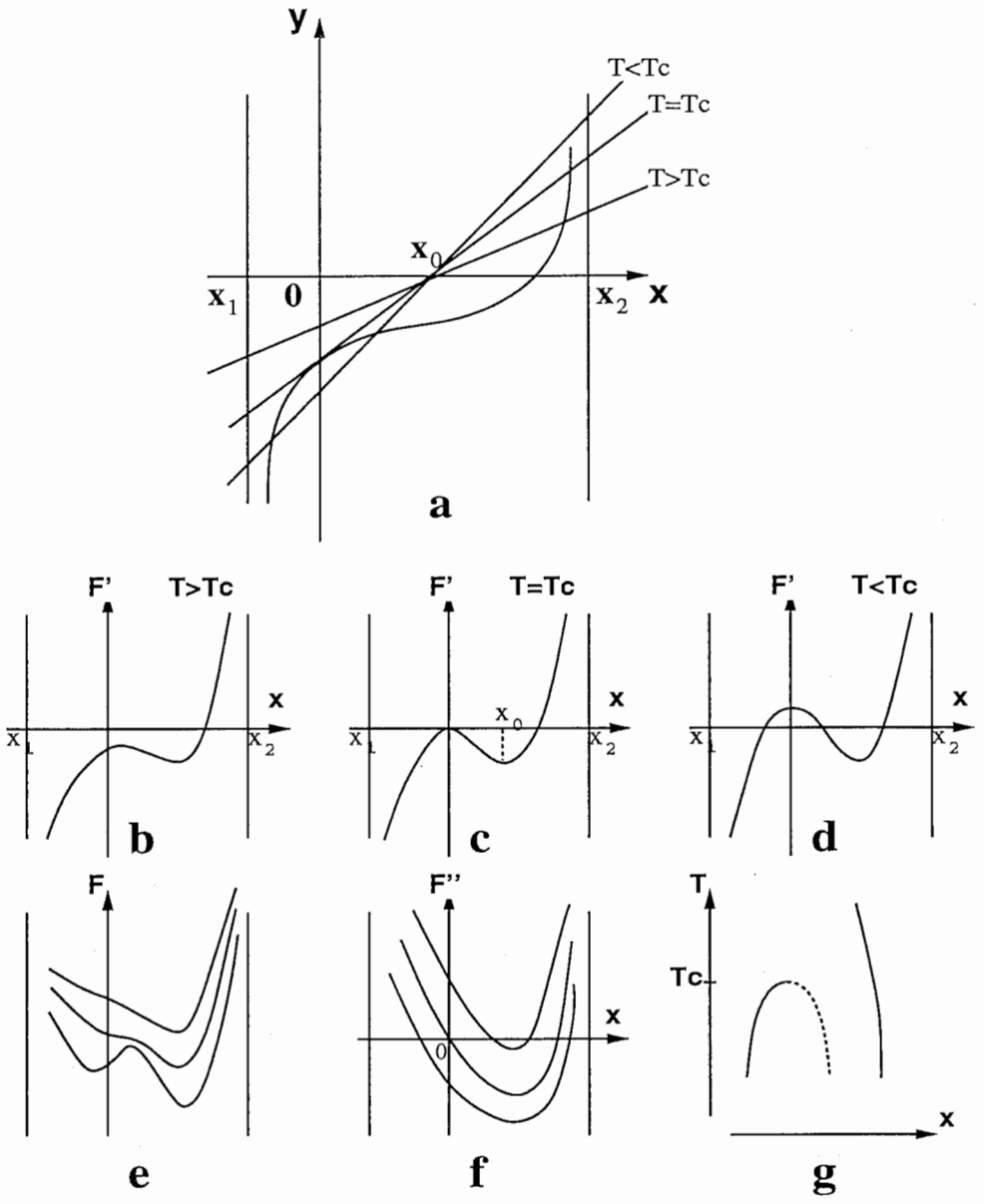

Figure 2 Saddle-node bifurcation.
A new minimum appears at the bifurcation point.

A saddle-node bifurcation that generates a new local minimum. (a) Two graphs, $y = dH/dx$, and $y = \eta(x - x_0)/T$ for $T < T_c$, $T = T_c$, and $T > T_c$, are shown. (b) The graph of $(\partial F/\partial x)$ for $T > T_c$. There is only one minimum. (c) The graph of $(\partial F/\partial x)$ for $T = T_c$. A new stationary point is generated. (d) The graph of $(\partial F/\partial x)$ for $T < T_c$. There are three stationary points; two are minima and the other is a saddle-point. (e) The graphs of F for $T > T_c$, $T = T_c$, and $T < T_c$. (f) The graphs of $(\partial^2 F/\partial x^2)$. At the bifurcation point, i.e., $T = T_c$ and $x = 0$, the free energy curvature is 0. (g) A new minimum and an unstable saddle point are born at $T = T_c$ beside the existing minima as the temperature decreases.

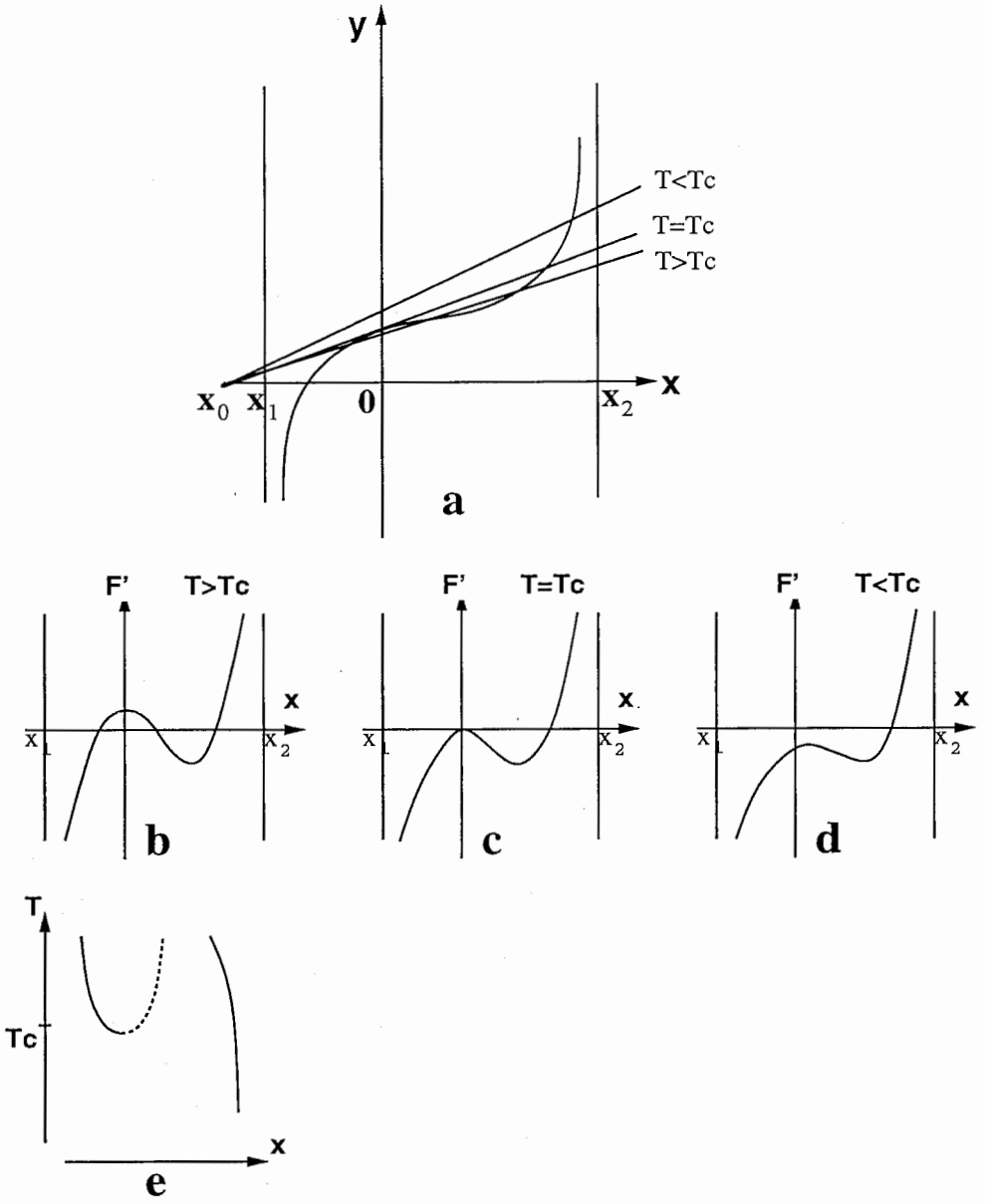

Figure 3 Saddle-node bifurcation.
A minimum disappears at the bifurcation point.

A saddle-node bifurcation that annihilates a local minimum and a saddle point. (a) Two graphs, $y = dH/dx$, and $y = \eta(x - x_0)/T$ for $T < T_c$, $T = T_c$, and $T > T_c$, are shown. (b) The graph of $(\partial F/\partial x)$ for $T > T_c$. There are three stationary points; two are minima and the other is a saddle-point. (c) The graph of $(\partial F/\partial x)$ for $T = T_c$. The minima and the saddle point collide with each other. (d) The graph of $(\partial F/\partial x)$ for $T < T_c$. There is only one minimum. (e) A minimum and a saddle point collide with each other at $T = T_c$ beside the existing minima and are annihilated as the temperature decreases.

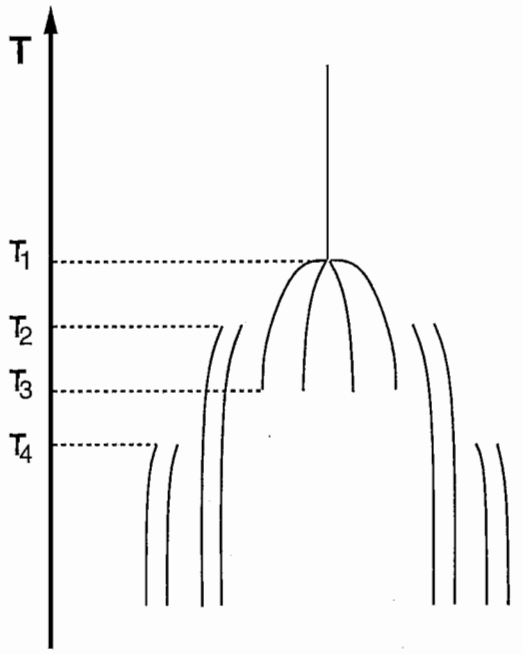

Figure 1

Schematic figure of the MFT bifurcation processes. The abscissa denotes the value of a state variable, and the ordinate denotes the temperature. The unique symmetric minimum at high temperature bifurcates into equivalent minima without cyclic symmetry through a cyclic symmetry breaking bifurcation at $T = T_1$, and is annihilated through a reverse symmetry breaking bifurcation at $T = T_3$. Besides them, new minima are generated by saddle-node bifurcations $T = T_2$ and $T = T_4$.

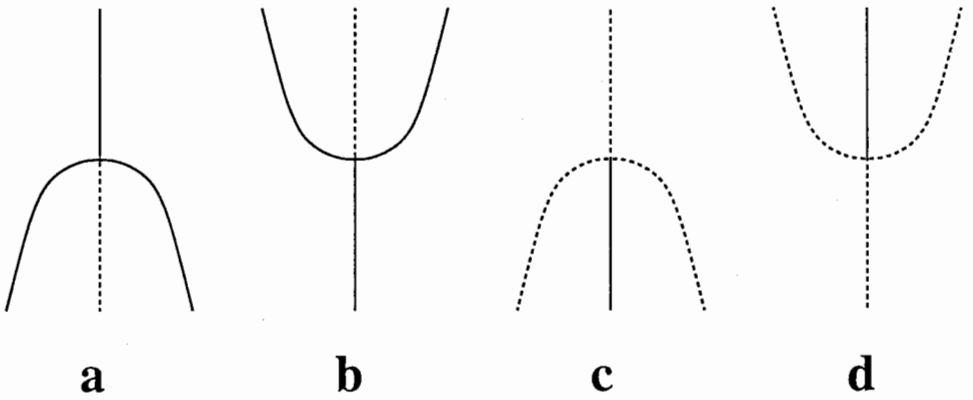

Figure 4

A reverse symmetry breaking bifurcation. The abscissa denotes the value of a state variable, and the ordinate denotes the temperature. The upper side of each figure denotes high temperature. The solid line and dotted line denote a stable stationary point (minimum) and an unstable stationary point (saddle point), respectively. The straight line and curved line denote a stationary point with reverse symmetry and without reverse symmetry, respectively.

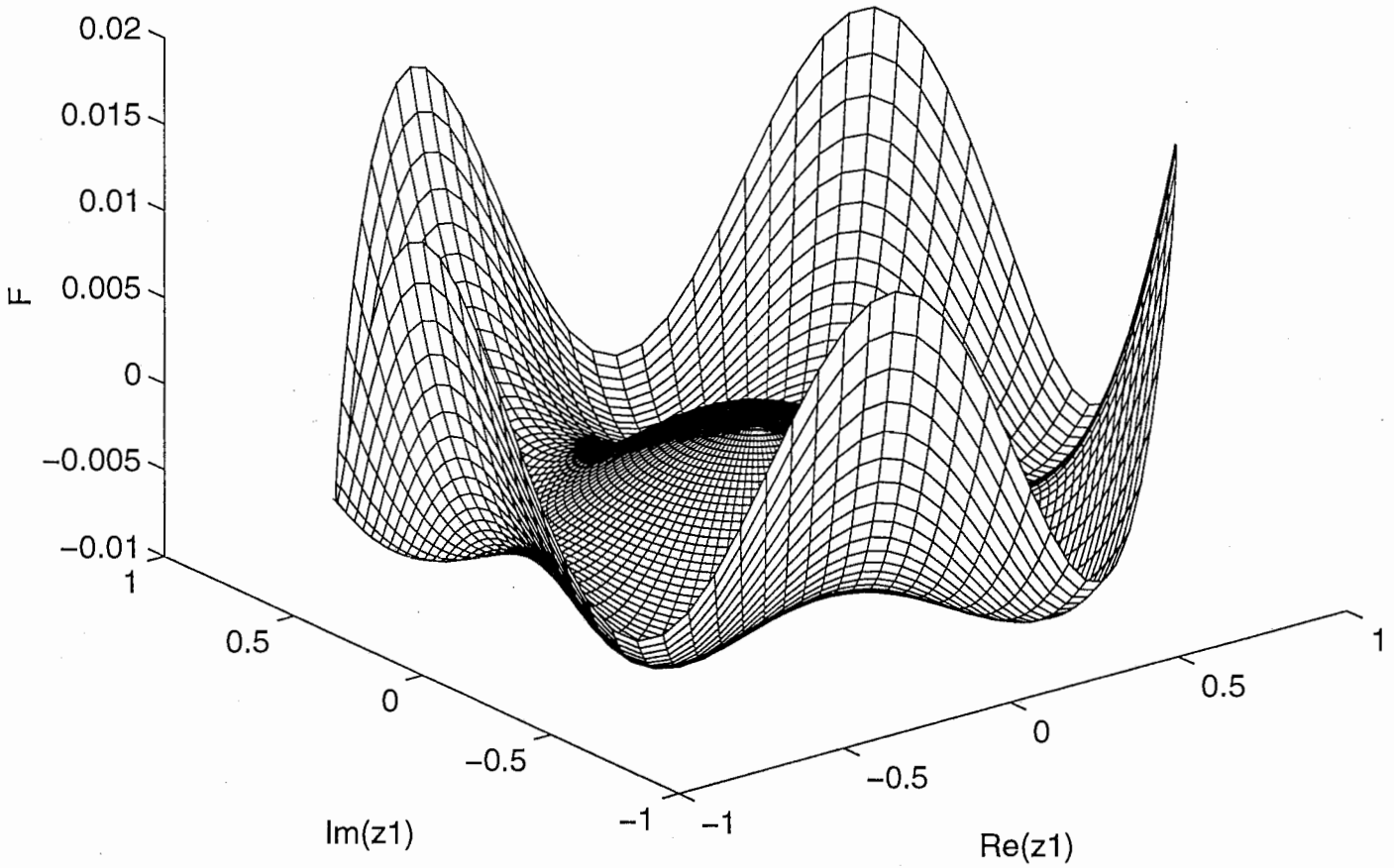

Figure 5

The shape of the effective free energy, Eq. (5.19), on a 2-dimensional subspace composed by two eigenvectors that correspond to the zero eigenvalue mode. Five minima without cyclic symmetry, five saddle points without cyclic symmetry, and a saddle point with cyclic symmetry can be observed. Stationary points without cyclic symmetry are located on the circle whose diameter is γ.

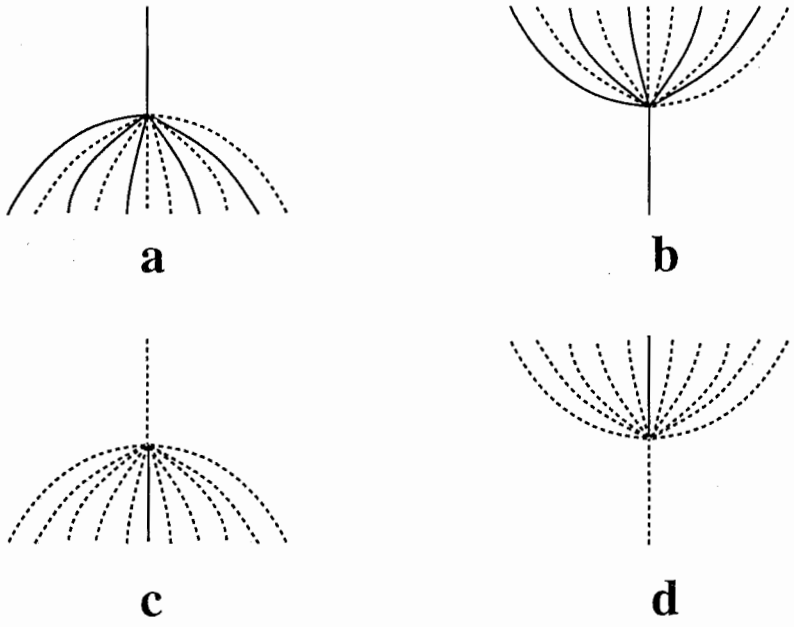

Figure 6

A cyclic symmetry breaking bifurcation. The abscissa denotes the value of a state variable, and the ordinate denotes the temperature. The upper side of each figure denotes high temperature. The solid line and dotted line denote a stable stationary point (minimum) and an unstable stationary point (saddle point), respectively. The straight line and curved line denote a stationary point with the N-th order cyclic symmetry, and a stationary point with the Q-th order cyclic symmetry, respectively, where $N = R \cdot Q$. In this figure, $N = 5$ and $Q = 1$.

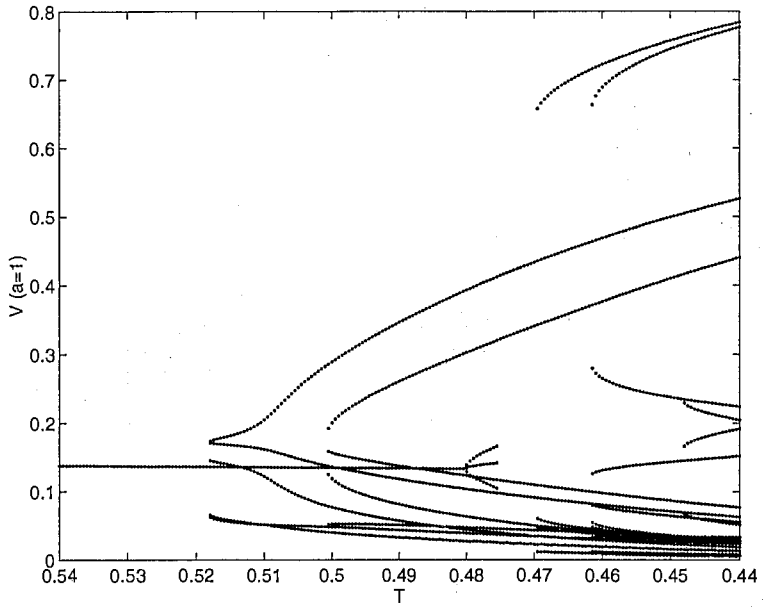

Figure 7(a)

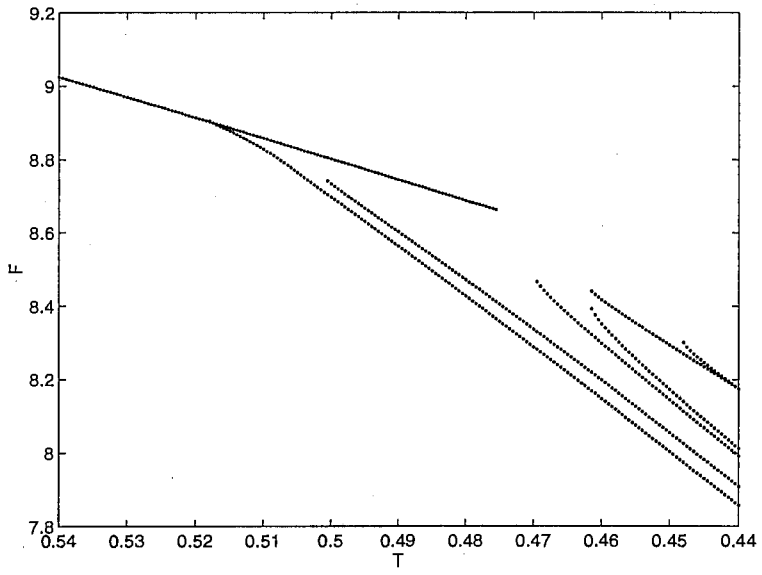

Figure 7(b)

(a) A typical example of a 5-city TSP bifurcation diagram, where $V_{1,i}$ $(i = 1, ..., 5)$ for every minimum are plotted against temperature. (b) The corresponding free energy diagram.